

---

# Estimating Long-term Heterogeneous Dose-response Curve: Generalization Bound Leveraging Optimal Transport Weights

---

Ze Qin Yang<sup>1,4\*</sup> Weilin Chen<sup>1\*</sup> Ruichu Cai<sup>1,2†</sup> Yuguang Yan<sup>1</sup> Zhifeng Hao<sup>3</sup>  
 Zhipeng Yu<sup>4</sup> Zhichao Zou<sup>4</sup> Jixing Xu<sup>4</sup> Peng Zhen<sup>4</sup> Jiecheng Guo<sup>4</sup>

<sup>1</sup> School of Computer Science, Guangdong University of Technology

<sup>2</sup> Pazhou Laboratory (Huangpu)

<sup>3</sup> College of Science, Shantou University

<sup>4</sup> Didi Chuxing

{youngzeqin, chenweilin.chn, cairuichu}@gmail.com

ygyan@gdut.edu.cn, haozhifeng@stu.edu.cn

{yuzhipeng, zouzichao, stevenxujixing, zhenpeng, jasanguo}@didiglobal.com

## Abstract

Long-term treatment effect estimation is a significant but challenging problem in many applications. Existing methods rely on ideal assumptions, such as no unobserved confounders or binary treatment, to estimate long-term average treatment effects. However, in numerous real-world applications, these assumptions could be violated, and average treatment effects are insufficient for personalized decision-making. In this paper, we address a more general problem of estimating long-term Heterogeneous Dose-Response Curve (HDRC) while accounting for unobserved confounders and continuous treatment. Specifically, to remove the unobserved confounders in the long-term observational data, we introduce an optimal transport weighting framework to align the long-term observational data to an auxiliary short-term experimental data. Furthermore, to accurately predict the heterogeneous effects of continuous treatment, we establish a generalization bound on counterfactual prediction error by leveraging the reweighted distribution induced by optimal transport. Finally, we develop a long-term HDRC estimator building upon the above theoretical foundations. Extensive experiments on synthetic and semi-synthetic datasets demonstrate the effectiveness of our approach.

## 1 Introduction

Long-term treatment effect estimation is practically significant in various domains [25, 19, 12]. While Randomized Controlled Trials (RCTs) are the gold standard for estimating causal effects, collecting long-term outcomes through RCTs is often infeasible due to high costs, e.g., it may take years or even decades to collect mortality outcomes in clinical trials. As a result, only short-term experimental data are typically available. In contrast, long-term observational data are often more accessible and cost-effective, and thus are commonly taken as a complement to short-term experimental data.

Under such data combination setting, there has been growing interest in leveraging short-term outcomes to assist in inferring long-term effects. With all observed confounders, to estimate long-term average effects, [29] studies the efficiency gains of incorporating the short-term outcomes from experimental data with only limited long-term outcomes under binary treatments, while [74]

---

\*Equal contributions

†Corresponding authors.

extends this to continuous treatments. As a counterpart, allowing for unobserved confounders, [3, 21, 26, 27] propose different assumptions to use short-term outcomes from experimental data to remove confounding in long-term observational data. Nevertheless, they still focus on long-term average effects of binary treatment.

Therefore, previous works lack practical applicability, since they have largely focused on estimating long-term average effects under ideal assumptions, e.g., no unobserved confounders in observational data or binary treatment setting. In practice, to develop personalized policies, decision-makers usually require long-term individual effects estimated with unobserved confounders and continuous treatment, where the average treatment effects are insufficiently informative and the above assumptions are easily violated. Consider a vocational training example where a company wants to evaluate the effect of training hours (*continuous treatment*) on one-year employment income (*long-term outcome*) of different participants (*heterogeneity*). To support this, two types of data can be collected: short-term experimental data that only collect multiple post-training skill assessment scores (*short-term outcomes*), and long-term historical observational data that contain both short- and long-term outcomes but suffer from unobserved confounders, such as participants' learning aptitude. In such a scenario, how to estimate the individual treatment effect of training hours on the long-term income of a specific participant, i.e., long-term Heterogeneous Dose-Response Curve (HDRC), still remains challenging.

Motivated by the example, this paper focuses on estimating long-term HDRC with unobserved confounders and continuous treatment via data combination, which presents two key challenges. First, the long-term outcome only exists in the observational data, suffering from unobserved confounders, and is missing in the experimental data, causing the identification problem. Second, the spaces of short- and long-term counterfactual outcomes are infinite since the treatment is continuous, causing a large counterfactual prediction error in estimating the long-term HDRC with only the actual outcome.

To address the first challenge of identifiability, we theoretically demonstrate that unobserved confounders can be eliminated by aligning the conditional distributions of short-term outcomes between observational and experimental data. To achieve such alignment, under the Optimal Transport (OT) reweighting framework, we establish a mini-batch and joint distribution-based upper bounds on the discrepancy of conditional distributions, which is computationally efficient and can be easily embedded into deep learning. Further, to address the second challenge of lacking counterfactual outcomes, we derive a generalization bound of counterfactual regression based on the reweighted distribution induced by optimal transport, showing the counterfactual prediction error of the long-term HDRC can be bounded by the observed weighted factual error with a weighted IPM term. Based on the above theoretical results, we propose our model called Long-term hEterogeneous dose-response curve estimAtor with Reweighting and represeNtation learning (LEARN), capable of reducing the observed and unobserved confounding bias. Our contributions are summarized as follows:

- To the best of our knowledge, this is the first work to address the problem of estimating long-term HDRC with unobserved confounders and continuous treatment via data combination.
- We theoretically show that the unobserved confounders can be removed by aligning the conditional distributions between observational and experimental data, and propose a practical and computationally OT weighting method to achieve such alignment.
- Based on the OT-induced reweighted distribution, we derive the generalization bound on the counterfactual prediction error in long-term HDRC estimation, which inspires our model.
- We conduct extensive experiments on multiple synthetic and semi-synthetic datasets to demonstrate the effectiveness of our proposed method.

## 2 Related Work

**Long-term Causal Inference.** A common strategy for long-term causal inference is to leverage short-term outcomes via data combination. Under the surrogacy assumption that short-term outcomes fully mediate the effect of treatment, [2] combines multiple short-term outcomes to robustly estimate the long-term average effects, [11] models the relationship between the short- and long-term outcomes via deep learning, [50] proposes kernel estimator for more complex average causal estimands and avoids linearity and separability assumptions. However, the surrogacy assumption is often too strong and may be violated in practice. With all observed confounders, [29] investigates the role of short-term outcomes for long-term causal inference under binary treatment, while [74] serves as

a counterpart for continuous treatment. [9] consider settings with partially unobserved surrogates and employ identifiable variational autoencoder for recovery. [56] address dynamic treatments through reinforcement learning, and [72, 67] develop policy learning method for balancing short- and long-term rewards. Further, to address the unobserved confounders, [3] introduces a relaxed latent unconfoundedness assumption to achieve identification, which is further leveraged by [10] to develop a doubly robust estimator. Alternative identifiability assumptions are proposed by [21, 26, 41]. Interestingly, [43] studies the bracketing relationship between identifiability assumptions in [3] and [21]. Based on proximal methods[53], [27] exploits the sequential structure of short-term outcomes. [58] performs instrumental variable regression to estimate long-term effects. Despite these advances across various settings, to the best of our knowledge, we are the first to focus on the long-term HDRC estimation problem with unobserved confounders and continuous treatment.

For other related work about dose-response curve and optimal transport, please refer to Appendix B.

### 3 Preliminary

#### 3.1 Optimal Transport Weighting

Optimal Transport (OT) [61] is widely used to quantify distribution discrepancy as the minimum cost of transporting one distribution to another. Among the rich theory of OT, we focus on the *Kantorovich Problem* [30] for discrete distribution in this paper. Recently, thanks to its many advantages, such as geometric sensitivity and stability, OT has been explored for learning weights to align distribution [18, 24, 71]. Specifically, suppose we want to learn weights  $\mathbf{w}_\alpha$  for samples in distribution  $\alpha$ , such that the reweighted distribution is aligned with another distribution  $\beta$ . To achieve this goal, we view the to-be-learned weights  $\mathbf{w}_\alpha$  as the probability measure of distribution  $\alpha$ , and represent the distribution  $\beta$  with a uniform probability measure  $\boldsymbol{\mu}$ . By doing so, the learning of  $\mathbf{w}_\alpha$  can be formulated as the process of minimizing the OT distance between distributions  $\alpha$  and  $\beta$ :

$$\begin{aligned} \min_{\mathbf{w}_\alpha} OT(\alpha, \beta) &= \min_{\mathbf{w}_\alpha} \min_{\Gamma \in \Pi(\alpha, \beta)} \langle \Gamma, C \rangle, \\ \text{s.t. } \Pi(\alpha, \beta) &= \{\Gamma \in \mathbb{R}^{n \times m} \mid \Gamma \mathbf{1}_m = \mathbf{w}_\alpha, \Gamma^T \mathbf{1}_n = \boldsymbol{\mu}, \Gamma_{ij} \in [0, 1]\}, \end{aligned} \quad (1)$$

where  $\langle \cdot, \cdot \rangle$  is the Frobenius inner product,  $n$  and  $m$  are the sample numbers of  $\alpha$  and  $\beta$ , the transport cost matrix  $C$  is the unit-wise distance between  $\alpha$  and  $\beta$ , the transport probability matrix  $\Gamma$  satisfying  $\Pi(\alpha, \beta)$  is learned by minimizing  $OT(\alpha, \beta)$ , which reflects how to transport samples from  $\alpha$  to  $\beta$ .

#### 3.2 Long-term Heterogeneous Dose-response Curve

Let  $A \in \mathcal{A}$  be the 1-dimensional continuous treatment,  $\mathbf{X} \in \mathcal{X}$  be the observed confounders,  $\mathbf{U} \in \mathcal{U}$  be the unobserved confounders,  $\mathbf{S}(a) \in \mathcal{S}$  be the potential short-term outcomes measured at timesteps  $1, 2, \dots, t_0$ , and  $Y(a) \in \mathcal{Y}$  be the potential long-term outcome measured at timestep  $T$ . Let lowercase letters (e.g.,  $a, \mathbf{x}, \mathbf{u}, \mathbf{s}(a), y(a)$ ) denote the value of the random variables. Following potential outcome framework [46], the observed short- and long-term outcomes  $\mathbf{S}, Y$  are the potential outcomes  $\mathbf{S}(a), Y(a)$  corresponding to the actually received treatment  $a$ .

Following [3, 10, 21], we consider a data combination setting where  $G = \{o, e\}$  distinguishes between two types of data: a large observational data  $O = \{a_i, \mathbf{x}_i, \mathbf{s}_i, y_i, G_i = o\}_{i=1}^{n_o}$  and a small experimental data  $E = \{a_i, \mathbf{x}_i, \mathbf{s}_i, G_i = e\}_{i=1}^{n_e}$  ( $n_e \ll n_o$ ). That is, the treatment  $A$ , covariates  $\mathbf{X}$  and short-term outcomes  $\mathbf{S}$  are available in both datasets, while long-term outcome  $Y$  is only available in the observational data. Our goal is to estimate the long-term Heterogeneous Dose-Response Curve (HDRC), which is defined as follows:

$$\mu(\mathbf{x}, a) = \mathbb{E}[Y(a) \mid \mathbf{X} = \mathbf{x}]. \quad (2)$$

Notably, the long-term HDRC cannot be estimated solely from the experimental data due to the missingness of long-term outcome  $Y$ , and also cannot be estimated solely from the observational data due to the possible unobserved confounders  $\mathbf{U}$ . To overcome these challenges, we learn long-term HDRC via data combination, requiring the following assumptions:

**Assumption 1** (Consistency). *If  $A = a$ , then  $Y = Y(a)$ ,  $\mathbf{S} = \mathbf{S}(a)$ .*

**Assumption 2** (Positivity).  $0 < P(A = a \mid \mathbf{X} = \mathbf{x}) < 1$ ,  $0 < P(G = o \mid A = a, \mathbf{X} = \mathbf{x}) < 1$ ,  $\forall a, \mathbf{x}$ .

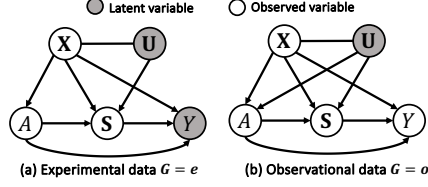


Figure 1: Causal graphs of experimental and observational data.

**Assumption 3** (Weak internal validity of observational data).  $A \perp\!\!\!\perp \{Y(a), \mathbf{S}(a)\} | \mathbf{X}, \mathbf{U}, G = o$  and  $A \not\perp\!\!\!\perp \{Y(a), \mathbf{S}(a)\} | \mathbf{X}, G = o$ .

**Assumption 4** (Internal validity of experimental data).  $A \perp\!\!\!\perp \{Y(a), \mathbf{S}(a)\} | \mathbf{X}, G = e$ .

**Assumption 5** (Unconfounded selection).  $G \perp\!\!\!\perp \{Y(a), \mathbf{S}(a)\} | \mathbf{X}$ .

**Assumption 6** (Latent unconfoundedness).  $A \perp\!\!\!\perp Y(a) | \mathbf{X}, \mathbf{S}(a), G = o$ .

The assumptions above are mild and widely used in existing literature, e.g., [3, 21]. Assumption 1 and 2 are standard assumptions in causal inference. Assumption 3 allows unobserved confounders to exist in observational data, which is much weaker than the classic unconfoundedness assumption. However, this assumption also poses challenges for identification because we cannot directly control all confounders  $\mathbf{X}, \mathbf{U}$  in practice. Different from Assumption 3, Assumption 4 does not allow for the presence of unobserved confounders in experimental data. Assumption 5 allows us to generalize the distribution of potential outcomes between different types of data  $G$ , and this assumption is reasonable because the difference between experimental and observational data is usually the treatment mechanism, while the potential outcome distributions remain unchanged and stable. Finally, Assumption 6 is the key assumption in our paper, which is first proposed by [3] to achieve long-term average effect identification under the binary-treatment setting. Different from [3], we reuse this assumption to identify long-term HDRC by a novel reweighting schema. This assumption means that unobserved confounders in the observational data is mediated through the short-term outcomes, effectively blocking the path  $\mathbf{U} \rightarrow Y$ . In our vocational training example, this assumption means that the short-term skill assessment scores fully reflect the participants’ learning aptitude. The causal graphs that satisfy the above assumptions are shown in Fig. 1.

## 4 Proposed Method

To estimate long-term HDRC unbiasedly, we address unobserved confounders via reweighting and observed confounders via representation learning, as detailed in Sections 4.1 and 4.2, respectively.

### 4.1 Optimal Transport Weights for Unobserved Confounders via Data Combination

We now present our method for handling the unobserved confounders in observational data. In section 4.1.1, we propose a novel reweighting schema dealing with the unobserved confounders in observational data, making long-term HDRC identifiable. In section 4.1.2, we provide a practical and computationally OT method to learn such weights via data combination.

#### 4.1.1 Identifiable Long-term HDRC via Reweighting

Since  $Y$  is only observed in observational data, identifying long-term HDRC requires the unconfoundedness assumption of observational data, i.e.,  $A \perp\!\!\!\perp \{\mathbf{S}(a), Y(a)\} | \mathbf{X}, G = o$ , which does not hold due to Assumption 3. Fortunately,  $A \perp\!\!\!\perp \{\mathbf{S}(a), Y(a)\} | \mathbf{X}, G = e$  holds, though  $Y$  is missing in the experimental data. It raises a question: can we remove the influence of unobserved confounders in the observational data to achieve identification, by utilizing experimental data that only includes short-term outcomes? We find that, although  $\mathbf{U}$  is unobserved, its influence can be captured by the (in)dependence between  $\mathbf{S}$  and  $G$  conditional on  $\mathbf{X}$  and  $A$ , as illustrated in the Proposition 1. For simplify, we denote  $P^{\mathbf{w}}(\cdot) = \mathbf{w}P(\cdot)$  as the reweighted distribution built on weights  $\mathbf{w}$ .

**Proposition 1.** *Under Assumptions 1, 2, 3, 4, 5, and 6, given a set of weights  $\mathbf{w} = \{\mathbf{w}_o, \boldsymbol{\mu}\}$  consisting of the learnable weights  $\mathbf{w}_o$  for observational units and uniform weights  $\boldsymbol{\mu}$  for experimental units, which makes  $P^{\mathbf{w}}(\mathbf{S}, G | \mathbf{X}, A) = P^{\mathbf{w}}(\mathbf{S} | \mathbf{X}, A)P^{\mathbf{w}}(G | \mathbf{X}, A)$ , i.e.,  $\mathbf{S} \perp\!\!\!\perp G | \mathbf{X}, A$ , then  $\mathbb{E}_{P^{\mathbf{w}}}[\mathbf{S}(a) | \mathbf{X}, A = a, G = o] = \mathbb{E}_{P^{\mathbf{w}}}[\mathbf{S}(a) | \mathbf{X}, G = o]$  holds.*

The proof is given in Appendix A.1. Proposition 1 is intuitive. Since unconfoundedness holds in  $G = e$ , then  $P(\mathbf{S}(a)|\mathbf{X}, G = e) = P(\mathbf{S}|\mathbf{X}, A = a, G = e)$ , but it does not hold when  $G = o$ . If we can learn weight  $\mathbf{w}$  aligning short-term outcomes between observational data and experimental data, i.e., making  $P(\mathbf{S}|\mathbf{X}, A, G = e) = P(\mathbf{S}|\mathbf{X}, A, G = o)$ , the unconfoundedness will also hold in  $G = o$  based on Assumption 5. Based on Proposition 1, we can further show the long-term HDRC is identifiable as follows.

**Theorem 1.** *Suppose assumptions in Proposition 1 hold, we have the unconfoundedness  $\mathbb{E}_{P^{\mathbf{w}}}[Y(a)|\mathbf{X}, A = a, G = o] = \mathbb{E}_{P^{\mathbf{w}}}[Y(a)|\mathbf{X}, G = o]$ , then the long-term HDRC can be identified.*

The proof is given in Appendix A.2. Theorem 1 is built on Proposition 1, indicating that if we could learn suitable weights making  $\mathbf{S} \perp\!\!\!\perp G|\mathbf{X}, A$ , the influence of unobserved confounders will be removed, and then long-term HDRC can be identified. Therefore, our goal now is to learn a set of weights  $\mathbf{w}_o$  for observational samples such that the conditional independence  $\mathbf{S} \perp\!\!\!\perp G|\mathbf{X}, A$  holds based on the reweighted distribution, i.e.,  $P^{\mathbf{w}_o}(\mathbf{S}|\mathbf{X}, A, G = o) = P^\mu(\mathbf{S}|\mathbf{X}, A, G = e)$ .

#### 4.1.2 Learning Optimal Transport Weights

Based on the above theoretical analyses, we need learn weights  $\mathbf{w}_o$  for observational samples to minimize the distances between  $P(\mathbf{S}|\mathbf{X}, A, G = o)$  and  $P(\mathbf{S}|\mathbf{X}, A, G = e)$ . However, most existing works only study how to measure the distances between joint distributions, instead of conditional distributions. Surprisingly, we find that under the optimal transport framework, the distance between conditional distributions can be bounded by that of joint distributions. As a result, we propose a mini-batch joint distribution-based OT method that not only helps align the conditional distributions but also can be easily embedded into the training of deep learning with theoretical guarantees.

To begin with, following Eq. (1), our goal is estimating weights  $\mathbf{w}_o$  for observational samples via minimizing the *conditional OT distance*, i.e.,  $OT(P(\mathbf{S}|\mathbf{X}, A, G = o), P(\mathbf{S}|\mathbf{X}, A, G = e))$ . The intuitive approach to solve this problem is to minimize every sub-problem  $OT(P(\mathbf{S}|\mathbf{X} = \mathbf{x}, A = a, G = o), P(\mathbf{S}|\mathbf{X} = \mathbf{x}, A = a, G = e))$  for every realization  $\mathbf{X} = \mathbf{x}, A = a$  as follows:

$$OT_{\mathbf{x},a}^{con} = \sum_{\mathbf{x},a} OT(P(\mathbf{S}|\mathbf{X} = \mathbf{x}, A = a, G = o), P(\mathbf{S}|\mathbf{X} = \mathbf{x}, A = a, G = e)). \quad (3)$$

**The First Challenge.** However, solving the above conditional OT problem is infeasible. The reason is that the conditional set  $(\mathbf{X}, A)$  are multi-dimensional continuous variables, leading to the existence of infinitely sub-problems in Eq. (3). To overcome this challenge, we establish a connection between the OT distance regarding conditional distributions and that regarding joint distributions:

**Theorem 2.** *Assuming the cost matrix of the joint distribution  $P(\mathbf{S}, \mathbf{X}, A)$  is separable, i.e.,  $C(\mathbf{s}, \mathbf{x}, a; \tilde{\mathbf{s}}, \tilde{\mathbf{x}}, \tilde{a}) = C(\mathbf{s}; \tilde{\mathbf{s}}) + C(\mathbf{x}; \tilde{\mathbf{x}}) + C(a; \tilde{a})$ , we have:*

$$OT_{\mathbf{x},a}^{con} \leq OT(P(\mathbf{S}, \mathbf{X}, A|G = o), P(\mathbf{S}, \mathbf{X}, A|G = e)). \quad (4)$$

*In addition, with assumption  $P(\mathbf{S} = \mathbf{s}, \mathbf{X} = \mathbf{x}, A = a|G = g) > 0$ , we have  $OT(P(\mathbf{S}, \mathbf{X}, A|G = o), P(\mathbf{S}, \mathbf{X}, A|G = e)) \rightarrow 0$  as  $n_o \rightarrow \infty$ , leading to  $OT_{\mathbf{x},a}^{con} \rightarrow 0$ .*

The proof can be found in Appendix A.3. The separable assumption is widely used to simplify the optimal transport problem [15, 34], and many distances such as the Manhattan distance and the squared Euclidean distance are separable. Theorem 2 shows that the conditional OT distance can be bounded by the OT distance between the corresponding joint distributions, which motivates us to learn weights  $\mathbf{w}_o$  by minimizing the upper bound  $OT(P(\mathbf{S}, \mathbf{X}, A|G = o), P(\mathbf{S}, \mathbf{X}, A|G = e))$  instead of the infeasible  $OT_{\mathbf{x},a}^{con}$ . And when  $n_o \rightarrow \infty$ ,  $OT_{\mathbf{x},a}^{con} \rightarrow 0$  means that the probability measure  $\mathbf{w}_o$  of the observational distribution  $P^{\mathbf{w}_o}(\mathbf{S}|\mathbf{X}, A, G = o)$  will converge to that of experimental distribution  $P(\mathbf{S}|\mathbf{X}, A, G = e)$ , ensuring HDRC identifiable based on Proposition 1.

**The Second Challenge.** While we solve the problem of conditional OT, another challenge about intensive computation emerges. Specifically, solving  $OT(P(\mathbf{S}, \mathbf{X}, A|G = o), P(\mathbf{S}, \mathbf{X}, A|G = e))$  will cause a high computational cost since the whole optimized transport matrix  $\Gamma \in \mathbb{R}^{n_o \times n_e}$  at each iteration can be large with the large size of whole observational data  $n_o$ . Additionally, optimizing the whole matrix at each iteration is also not suitable for the mini-batch training manner of deep learning. To tackle this challenge, inspired by [73], we propose a mini-batch OT based on randomly sub-sampled observational data and provide its theoretical analysis as follows:

**Definition 1.** Consider two empirical distributions  $\alpha$  and  $\beta$  with  $n$  and  $m$  units, we assume the batch size  $b$  of the first distribution  $\alpha$  satisfy  $b \mid n$  and let  $k = n/b$  be the number of batches. Let  $\mathcal{B}_i$  be index set of the  $i$ -th batch in  $\alpha$  and the corresponding empirical distribution is  $\alpha_{\mathcal{B}_i}$ , then the mini-batch OT problem is defined as:

$$m\text{-}OT(\alpha, \beta) = \frac{1}{k} \sum_{i=1}^k OT(\alpha_{\mathcal{B}_i}, \beta). \quad (5)$$

**Theorem 3.** Let  $\gamma_i$  be the optimal transport probability matrix of the  $i$ -th batch OT problem of  $m\text{-}OT(P(\mathbf{S}, \mathbf{X}, A|G=o), P(\mathbf{S}, \mathbf{X}, A|G=e))$ . With extending  $\gamma_i$  to a  $n_o \times n_e$  matrix  $\Gamma_i$  that pads zero entries to the row whose index does not belong to  $\mathcal{B}_i$ , we have:

$$\frac{1}{k} \sum_{i=1}^k \Gamma_i \in \Pi(P(\mathbf{S}, \mathbf{X}, A|G=o), P(\mathbf{S}, \mathbf{X}, A|G=e)), \quad (6)$$

and

$$OT(P(\mathbf{S}, \mathbf{X}, A|G=o), P(\mathbf{S}, \mathbf{X}, A|G=e)) \leq m\text{-}OT(P(\mathbf{S}, \mathbf{X}, A|G=o), P(\mathbf{S}, \mathbf{X}, A|G=e)). \quad (7)$$

The proof is in Appendix A.4. Theorem 3 implies that the OT distance of the joint distribution  $P(\mathbf{S}, \mathbf{X}, A)$  between observational and experimental data is upper-bounded by its corresponding  $m\text{-}OT$  problem. Solving the  $m\text{-}OT$  problem not only significantly reduces the high optimization cost, but also allows us to embed the OT distance into the deep learning framework, where only batch observational units and full experimental units are considered at each training iteration.

**Conclusion.** We have overcome two challenges about the conditional OT distance and high computational cost via Theorem 2 and Theorem 3 respectively. Combining these two theorems, we could learn the weights  $\mathbf{w}_o$  by minimizing  $m\text{-}OT(P(\mathbf{S}, \mathbf{X}, A|G=o), P(\mathbf{S}, \mathbf{X}, A|G=e))$ , which is the upper bound of the original  $OT_{\mathbf{x},a}^{con}$ . As a result, our estimated weights  $\mathbf{w}_o$  could achieve Proposition 1 approximately, which leads to the identification of HDRC according to Theorem 1.

## 4.2 Generalization Bound on Long-term HDRC

Although the OT-induced weights  $\mathbf{w}_o$  could remove the unobserved confounders and makes HDRC identifiable, the counterfactual prediction error about long-term HDRC is still large. The reason is that the regression can only be trained with the factual outcomes while the counterfactual ones are infinite due to the continuous treatment, and the confounding bias exists since  $\mathbf{X} \not\perp A$ . To address it, we now derive the generalization bound about the counterfactual prediction error based on the OT-based reweighted distribution, where the unobserved confounding bias has been removed.

We first define some notations for discussion. Let  $\phi : \mathcal{X} \rightarrow \mathcal{Z}$  be a representation function with inverse  $\psi$ , where  $\mathcal{Z}$  is the representation space. Let  $g : \mathcal{Z} \times \mathcal{A} \rightarrow \mathcal{S}$  and  $h : \mathcal{Z} \times \mathcal{A} \times \mathcal{S} \rightarrow \mathcal{Y}$  be the hypotheses that predict the potential short- and long-term outcomes. Since we aims to predict potential long-term outcome  $Y(a)$  for all possible treatments  $a$  on sample  $\mathbf{x}$ , which requires that we could already predict the potential short-term outcomes  $\mathbf{S}(a)$  accurately. As a result, we define the combined loss for learning these two hypotheses  $g, h$  as  $\ell_{\phi, g, h}(\mathbf{x}, a) = \ell_{\phi, g}^s(\mathbf{x}, a) + \ell_{\phi, h}^y(\mathbf{x}, a)$ , where  $\ell_{\phi, g}^s(\mathbf{x}, a) = \int_{\mathcal{S}} L(\mathbf{s}(a), g(\phi(\mathbf{x}), a))P(\mathbf{s}(a)|\mathbf{x})d\mathbf{s}(a)$  and  $\ell_{\phi, h}^y(\mathbf{x}, a) = \int_{\mathcal{S} \times \mathcal{Y}} L(y(a), h(\phi(\mathbf{x}), a, \mathbf{s}(a)))P(y(a), \mathbf{s}(a)|\mathbf{x})d\mathbf{s}(a)dy(a)$  ( $L(\cdot, \cdot)$  is the error function). Therefore, the ideal prediction error over all treatment  $a$  for  $\mathbf{x}$  can be defined as  $\mathcal{E}(\mathbf{x}) = \mathbb{E}_{a \sim P(A)}[\ell_{\phi, g, h}(\mathbf{x}, a)]$ , and the target of counterfactual prediction is minimizing  $\mathcal{E}_{cf} = \mathbb{E}_{\mathbf{x} \sim P(\mathbf{X})}[\mathcal{E}(\mathbf{x})]$ .

However,  $\mathcal{E}_{cf}$  is practically incomputable, because the factual data we access lack the counterfactual outcomes. As a result, we can only obtain the prediction error on the reweighted factual distribution as  $\mathcal{E}_f^{\mathbf{w}_o} = \mathbb{E}_{\mathbf{x}, a \sim P^{\mathbf{w}_o}(\mathbf{X}, A)}[\ell_{\phi, g, h}(\mathbf{x}, a)]$ . Next, following [49, 6], we derive a generalization bound to bridge a connection between  $\mathcal{E}_{cf}$  and  $\mathcal{E}_f^{\mathbf{w}_o}$  in the long-term HRDC estimation scenario:

**Theorem 4.** Assuming a family  $\mathcal{M}$  of function  $m : \mathcal{Z} \times \mathcal{A} \rightarrow \mathbb{R}$ , and there exists a constant  $B_\Phi > 0$  such that  $\frac{1}{B_\Phi} \cdot \ell_{\phi, g, h}(\mathbf{x}, a) \in \mathcal{M}$ , then we have:

$$\mathcal{E}_{cf} \leq \mathcal{E}_f^{\mathbf{w}_o} + IPM_{\mathcal{M}}(P(\mathbf{Z})P(A), \mathbf{w}_o \cdot P(\mathbf{Z}, A)), \quad (8)$$

where  $IPM_{\mathcal{M}}(p, q) = \sup_{m \in \mathcal{M}} \left| \int_{\mathcal{X}} g(x)(p(x) - q(x))dx \right|$  is integral probability metric for a chosen  $\mathcal{M}$ ,  $P(\mathbf{Z})$  and  $P(\mathbf{Z}, A)$  are distributions induced by the map  $\phi$  from  $P(\mathbf{X})$  and  $P(\mathbf{X}, A)$ .

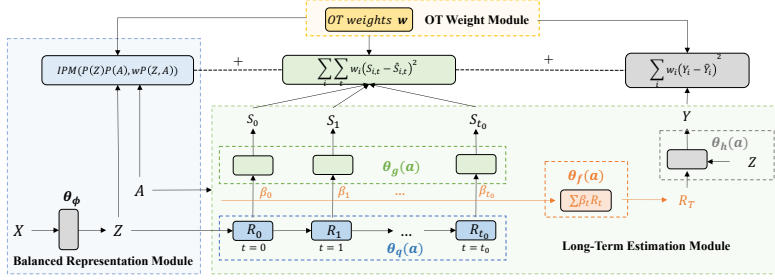


Figure 2: Model architecture of the proposed LEARN.

The proof is given in Appendix A.5. Theorem 4 states that the counterfactual error  $\mathcal{E}_{cf}$  is upper-bounded by the factual error  $\mathcal{E}_f^{\mathbf{w}_o}$  plus a reweighted IPM term that measures the dependence between treatment  $A$  and observed confounders  $\mathbf{X}$ . The theorem inspires a classical balanced representation method based on deep learning [49], which handles the observed confounding bias by learning the balanced representation  $\mathbf{Z} = \phi(\mathbf{X})$  that is independent of treatment  $A$ , i.e.,  $\mathbf{Z} \perp\!\!\!\perp A$ .

## 5 Model Architecture

We have presented the theoretical results, which handle the unobserved and observed confounders by reweighting and representation learning, respectively. In this section, we summarize the model architecture inspired by the theoretical results. As shown in Fig. 2, LEARN can be divided into three modules: OT weight module, balanced representation module and long-term estimation module.

**OT Weight Module.** Based on Theorems 2 and 3, we design this module to estimate weights  $\mathbf{w}_o$  for removing the unobserved confounding bias. To embed the  $m$ -OT( $\alpha, \beta$ ) problem into deep learning, following [73], we approximate it by solving  $OT(\alpha_{\mathcal{B}}, \beta)$  over each mini-batch  $\mathcal{B}$ . As a result, we learn the weights  $\mathbf{w}_{o,\mathcal{B}} = \{w_{o,1}, \dots, w_{o,b}\}$  by minimizing  $OT(P_{\mathcal{B}}(\mathbf{S}, \mathbf{X}, A|G=o), P(\mathbf{S}, \mathbf{X}, A|G=e))$  between the batch observational data and full experimental data at each iteration. However, optimizing the OT problem directly usually induces a sparse solution, which means only a limited number of observational units are transported, suffering from low data efficiency [8, 63]. Motivated by [71], we apply a negative entropy regularization on the marginal distributions  $\mathbf{w}_{o,\mathcal{B}}$ , i.e.,  $\Omega(\mathbf{w}_{o,\mathcal{B}}) = \sum_{j=1}^b w_{o,j}(\log w_{o,j} - 1)$ , to encourage more observational units to be transported, and also avoid the heavy computation of the linear programming [17]. Finally, we learn weights  $\mathbf{w}_{o,\mathcal{B}}$  as follows:

$$\begin{aligned} \min_{\mathbf{w}_{o,\mathcal{B}}} \min_{\gamma \in \Pi(\alpha_{\mathcal{B}}, \beta)} \langle \gamma, \mathbf{C} \rangle + \lambda_e \Omega(\gamma), \\ \text{s.t. } \Pi(\alpha_{\mathcal{B}}, \beta) = \{ \gamma \in \mathbb{R}^{b \times n_e} \mid \gamma \mathbf{1}_{n_e} = \mathbf{w}_{o,\mathcal{B}}, \gamma^T \mathbf{1}_b = \boldsymbol{\mu}, \gamma_{ij} \in [0, 1] \}, \end{aligned} \quad (9)$$

where  $\lambda_e$  is the hyperparameter and cost matrix  $\mathbf{C}$  is constructed based on the Euclidean distance.

Following [71], we develop a projected mirror descent [39, 45] to solve the problem (9), which firstly performs proximal gradient descent with the Bregman divergence [5], and then obtains a feasible solution in the set  $\Pi(\alpha_{\mathcal{B}}, \beta)$  by projection. The details can be found in Appendix A.6.

**Balanced Representation Module.** Based on Theorem 4, we design this module to correct the observed confounding bias. We transform the observed confounders  $\mathbf{X}$  into balanced representation  $\mathbf{Z}$  through MLP  $\phi(\cdot)$  with parameter  $\theta_\phi$  via minimizing  $IPM(P(\mathbf{Z})P(A), \mathbf{w}_{o,\mathcal{B}}P(\mathbf{Z}, A))$ . In practice, we use the Wasserstein distance [62] as the implementation of the IPM. To calculate it, we simulate samples standing for the product of marginal distributions  $P(\mathbf{Z})P(A)$  by randomly permuting the observed treatment  $A$ , and the original samples are drawn from the joint distribution  $P(\mathbf{Z}, A)$ .

**Long-Term Estimation Module.** This module aims to estimate the potential long-term outcome  $Y(a)$  based on potential short-term outcomes  $\mathbf{S}(a)$  for different units. We follow LTEE [11] to model the relationship between the short- and long-term outcomes. Specifically, the balanced representations  $\mathbf{Z}$  are firstly fed into the GRU  $q(\cdot)$  to obtain the short-term representations  $\mathbf{R}_t$  at each timestep  $t$ , which is then used to predict the corresponding short-term outcome  $\hat{S}_t$  with a shared MLP  $g(\cdot)$ . After that, we leverage the attention mechanism  $f(\cdot)$  [4] to construct the long-term representation  $\mathbf{R}_T$  from  $\{\mathbf{R}_1, \mathbf{R}_2, \dots, \mathbf{R}_{t_0}\}$ , and then predict the long-term outcome  $\hat{Y}_T$  through an MLP  $h(\cdot)$ .

However, different from the original LTEE which only works with binary treatment, we employ the varying coefficient structure [40] to extend this module to a continuous treatment scenario. In particular, we use splines to model the parameters  $\theta(\cdot)$  of the above four network structures  $q(\cdot), g(\cdot), f(\cdot), h(\cdot)$ . As a result, the influence of the treatment information is not lost in high-dimensional representations, which in practice has been shown to lead to better performance.

**Loss Function.** The training loss at each iteration of the above modules is:

$$\begin{aligned} \mathcal{L}_\theta = & \frac{1}{b} \sum_{i=1}^b w_{o,i} (y_i - \hat{y}_i)^2 + \frac{\lambda_o}{b} \sum_{i=1}^b \sum_{t=1}^{t_0} w_{o,i} (s_{i,t} - \hat{s}_{i,t})^2 + \frac{1 - \lambda_o}{n_e} \sum_{i=1}^{n_e} \sum_{t=1}^{t_0} (s_{i,t} - \hat{s}_{i,t})^2 \\ & + \lambda_b IPM(\{\phi(\mathbf{x}_i), \tilde{a}_i\}_{i=0}^b, \{w_{o,i}\phi(\mathbf{x}_i), w_{o,i}a_i\}_{i=0}^b), \end{aligned} \quad (10)$$

where  $\lambda_b$  is the strength of IPM, and  $\tilde{A}_i$  is the samples obtained by randomly permuting original treatment samples  $A_i$ . To make full use of the datasets, besides the observational data, we also train the model based on the prediction error of the short-term outcomes on experimental data, and use  $\lambda_o$  to control its strength. We provide more implementation details and the pseudocode in Appendix C.

## 6 Experiments

In this section, we conduct experiments to validate the effectiveness and correctness of our proposed model **LEARN**. In particular, we aim to answer the following research questions (RQs):

**RQ1:** How does LEARN perform in long-term HDRC estimation compared to existing methods?

**RQ2:** Do the designed modules effectively address both observed and unobserved confounding bias?

**RQ3:** How does batch size affect the approximation error about  $m$ -OT problem in Theorem 3?

**RQ4:** How does the size of experimental data used for data combination affect the performance?

**RQ5:** Does our model stably perform well under different choices of hyperparameters?

### 6.1 Experimental Setup

**Dataset Generation.** Since the true long-term HDRC is unavailable for real-world datasets, following prior works [40, 65, 32], we use five synthetic datasets with varying levels of unobserved confounding bias controlled by  $\beta_U \in \{1, 1.5, 2, 2.5, 3\}$ , and two semi-synthetic datasets, News [48] and TCGA [66], to evaluate our model. Details of the data generation are provided in Appendix D.1.

**Baselines.** We first compare our model with several baselines designed for continuous treatment, including **DRNet** [48], **VCNet** [40], **SCIGAN** [7], **ADMIT** [65] and **ACFR** [32]. Besides, since there is a lack of work on estimating long-term HDRC, we adapt LTEE [11] to the continuous treatment setting by incorporating a varying coefficient structure, denoted as **LTEE(VCNet)**. Moreover, to evaluate the contribution of each component in our model, we also include two ablated variants: **LEARN(None)** removes all modules addressing confounding bias; **LEARN(IPM)** includes only the IPM term to correct observed confounding bias, without accounting for the unobserved one.

**Metrics.** we first split the observational dataset with a 6/2/2 ratio into training, validation and test sets, and we report the mean integrated square error (MISE) and standard deviations over 5 independent replications on the test set:  $MISE = \frac{1}{n} \sum_{i=1}^n \int_{a_1}^{a_2} (\mu(\mathbf{x}_i, a) - \hat{\mu}(\mathbf{x}_i, a))^2 da$ , where  $n$  is the test sample size and  $[a_1, a_2]$  is the sampling interval of treatment values.

### 6.2 Result and Analysis

**Overall Performance (RQ1).** Table 1 presents the results on synthetic and semi-synthetic datasets, with the following key findings. Firstly, LEARN achieves the highest accuracy across all datasets, outperforming baselines only designed for continuous treatments. This improvement is attributed to the proposed long-term estimation module using attention mechanism to model the relationship between short- and long-term outcomes, which also benefit LTEE(VCNet). Secondly, LEARN(IPM) outperforms LEARN(None), indicating that minimizing the IPM term helps reduce observed confounding bias by learning balanced representations, thereby lowering MISE. Finally, LEARN further

Table 1: Results of HDRC estimation on five synthetic and two semi-synthetic datasets. The MISE is reported as Mean  $\pm$  Std. The best-performing method is bolded.

Dataset	Synthetic					News	TCGA
	$\beta_U = 1$	$\beta_U = 1.5$	$\beta_U = 2.0$	$\beta_U = 2.5$	$\beta_U = 3$		
DRNet	26.36 $\pm$ 7.32	28.98 $\pm$ 7.49	33.76 $\pm$ 8.75	39.35 $\pm$ 9.44	47.92 $\pm$ 10.47	1.975 $\pm$ 0.278	1.088 $\pm$ 0.517
SCIGAN	26.54 $\pm$ 6.98	30.52 $\pm$ 7.51	34.88 $\pm$ 8.44	40.45 $\pm$ 8.42	48.13 $\pm$ 9.73	2.450 $\pm$ 0.328	1.428 $\pm$ 1.219
VCNet	24.17 $\pm$ 7.21	27.93 $\pm$ 7.99	31.89 $\pm$ 8.95	36.43 $\pm$ 9.88	43.11 $\pm$ 11.24	1.524 $\pm$ 0.224	0.511 $\pm$ 0.616
ADMIT	23.01 $\pm$ 6.95	26.95 $\pm$ 6.80	30.76 $\pm$ 7.88	34.14 $\pm$ 8.62	41.39 $\pm$ 10.22	1.416 $\pm$ 0.173	0.496 $\pm$ 0.582
ACRF	22.93 $\pm$ 7.13	26.81 $\pm$ 6.57	30.72 $\pm$ 7.06	34.28 $\pm$ 7.20	41.01 $\pm$ 11.01	1.547 $\pm$ 0.276	0.534 $\pm$ 0.572
LTEE(VCNet)	22.63 $\pm$ 6.81	25.89 $\pm$ 6.49	29.95 $\pm$ 8.00	33.84 $\pm$ 8.37	40.25 $\pm$ 9.42	1.355 $\pm$ 0.167	0.471 $\pm$ 0.558
LEARN(None)	23.43 $\pm$ 7.42	26.38 $\pm$ 7.14	30.28 $\pm$ 8.25	34.09 $\pm$ 9.06	40.65 $\pm$ 10.33	1.360 $\pm$ 0.131	0.475 $\pm$ 0.561
LEARN(IPM)	22.61 $\pm$ 7.18	25.84 $\pm$ 6.65	29.76 $\pm$ 8.08	33.47 $\pm$ 8.44	39.89 $\pm$ 9.51	1.351 $\pm$ 0.134	0.468 $\pm$ 0.562
LEARN	<b>21.98 <math>\pm</math> 6.81</b>	<b>25.22 <math>\pm</math> 6.47</b>	<b>28.14 <math>\pm</math> 6.70</b>	<b>33.07 <math>\pm</math> 8.29</b>	<b>38.59 <math>\pm</math> 9.46</b>	<b>1.316 <math>\pm</math> 0.168</b>	<b>0.464 <math>\pm</math> 0.555</b>

surpasses LEARN(IPM), which highlights the importance of addressing unobserved confounding bias and verifies the effectiveness of our OT weight module.

**Confounding Bias Correction (RQ2).** Table 2 evaluates the effectiveness of our designed modules in correcting both observed and unobserved confounders on the synthetic dataset ( $\beta_U = 1$ ). **For observed confounders**, we assess the impact of the balanced representation module using the Hilbert-Schmidt Independence Criterion (HSIC, [22]). Results show an 83.45% reduction in the dependence between  $\phi(\mathbf{X})$  and  $A$ , indicating significantly mitigated observed confounding bias. **For unobserved confounders**, the effectiveness of the OT weight module is evaluated using the Hilbert-Schmidt Conditional Independence Criterion (HSCONIC, [20, 52]) to assess the unconfoundedness assumption in observational data after reweighting, i.e.,  $A \perp\!\!\!\perp \{Y(a), \mathbf{S}(a)\} | \mathbf{X}, G = o$ . We observe that reweighting reduces the conditional dependence between  $A$  and  $Y(a), \mathbf{S}(a)$  given  $\mathbf{X}$  by 71.55% and 67.71%, respectively, supporting the effectiveness of the OT weight module.

Table 2: Results of the model performance in reducing observed and unobserved confounding bias.

	Observed	Unobserved	
	HSIC( $\mathbf{X}, A$ )	HSCONIC( $\mathbf{S}(a), A   \mathbf{X}$ )	HSCONIC( $Y(a), A   \mathbf{X}$ )
Reduce ratio	83.45%	71.55%	67.71%

**Sensitivity of Batch Size (RQ3).** Following [51], we analyze the sensitivity of batch size in the  $m$ -OT problem by computing the relative approximation error:  $\frac{|m-OT_B(\alpha, \beta) - OT^*(\alpha, \beta)|}{OT^*(\alpha, \beta)}$ , where  $OT^*(\alpha, \beta) = \langle \Gamma^*, C \rangle$  is the optimal transport cost optimized using full observational data, and  $m-OT_B(\alpha, \beta)$  is the approximate cost with batch size  $B$ . Table 3 reports the results on synthetic dataset ( $\beta_U = 1$ ), which shows that smaller batches lead to higher relative approximation error, reflecting a trade-off between computational efficiency and accuracy about  $m-OT$  problem. However, even with the smallest batch size of 512, the relative error 14.51% is acceptable.

Table 3: The relative approximation error of different batch size about  $m-OT$  problem in Theorem 3.

Batch Size	512	1024	2048	4096
Relative Error	14.51%	7.68%	3.45%	1.03%

**Impact of Sample Size on experimental data (RQ4).** Since LEARN relies on data combination with experimental data, we evaluate the impact of the experimental sample size on MISE using the synthetic dataset ( $\beta_U = 1$ ). Results in Table 4 show that MISE decreases with larger sample sizes, as a larger experimental data provides a more reliable distribution for aligning the observational data, which allows us to learn more effective weights for eliminating unobserved confounding bias.

Table 4: The impact of experimental data’s sample size on the MISE of HDRC estimation.

Number	100	250	500	1000	2000
MISE	22.52 $\pm$ 7.40	22.18 $\pm$ 7.19	21.98 $\pm$ 6.81	21.63 $\pm$ 6.83	21.43 $\pm$ 6.74

**Hyperparameter Sensitivity Study (RQ5).** We investigate the impact of three hyperparameters  $\lambda_b, \lambda_o, \lambda_e$ . The details can be found in Appendix D.2.

## 7 Conclusion

In this paper, we provide a practical solution to estimate the long-term HDRC with unobserved confounders and continuous treatment via data combination, which is not well-studied in existing

work. Specifically, to remove unobserved confounders and make long-term HDRC identifiable, we first propose a novel weighting schema aligning the conditional distribution of short-term outcomes between observational and experimental groups. We solve the reweighting problem under an optimal transport framework, showing that the conditional distribution discrepancy can be bounded by mini-batch joint distribution discrepancy, which is computationally efficient. Further, to handle the observed confounders, we derive a generalization bound on the counterfactual outcome regression error based on the OT-induced reweighted distribution. Building upon the above theoretical results, we develop our model LEARN to estimate long-term HDRC accurately. Extensive experimental results verify the correctness of our theory and the effectiveness of LEARN.

## 8 Acknowledgments

This research was supported in part by National Science and Technology Major Project (2021ZD0111501), National Science Fund for Excellent Young Scholars (62122022), Natural Science Foundation of China (U24A20233, 62206064, 62206061, 62476163, 62406078), Guangdong Basic and Applied Basic Research Foundation (2023B1515120020), and CCF-DiDi GAIA Collaborative Research Funds (CCF-DiDi GAIA 202403).

## References

- [1] M. Arjovsky, S. Chintala, and L. Bottou. Wasserstein generative adversarial networks. In *International Conference on Machine Learning*, pages 214–223, 2017.
- [2] S. Athey, R. Chetty, G. W. Imbens, and H. Kang. The surrogate index: Combining short-term proxies to estimate long-term treatment effects more rapidly and precisely. Technical report, National Bureau of Economic Research, 2019.
- [3] S. Athey, R. Chetty, and G. Imbens. Combining experimental and observational data to estimate treatment effects on long term outcomes. *arXiv preprint arXiv:2006.09676*, 2020.
- [4] D. Bahdanau, K. Cho, and Y. Bengio. Neural machine translation by jointly learning to align and translate. *arXiv preprint arXiv:1409.0473*, 2014.
- [5] A. Banerjee, S. Merugu, I. S. Dhillon, J. Ghosh, and J. Lafferty. Clustering with bregman divergences. *Journal of machine learning research*, 6(10), 2005.
- [6] A. Bellot, A. Dhir, and G. Prando. Generalization bounds and algorithms for estimating conditional average treatment effect of dosage. *arXiv preprint arXiv:2205.14692*, 2022.
- [7] I. Bica, J. Jordon, and M. van der Schaar. Estimating the effects of continuous-valued interventions using generative adversarial networks. *Advances in Neural Information Processing Systems*, 33:16434–16445, 2020.
- [8] M. Blondel, V. Seguy, and A. Rolet. Smooth and sparse optimal transport. In *International conference on artificial intelligence and statistics*, pages 880–889. PMLR, 2018.
- [9] R. Cai, W. Chen, Z. Yang, S. Wan, C. Zheng, X. Yang, and J. Guo. Long-term causal effects estimation via latent surrogates representation learning. *Neural Networks*, page 106336, 2024.
- [10] J. Chen and D. M. Ritzwoller. Semiparametric estimation of long-term treatment effects. *Journal of Econometrics*, 237(2):105545, 2023.
- [11] L. Cheng, R. Guo, and H. Liu. Long-term effect estimation with surrogate representation. In *Proceedings of the 14th ACM International Conference on Web Search and Data Mining*, pages 274–282, 2021.
- [12] R. Chetty, J. N. Friedman, N. Hilger, E. Saez, D. W. Schanzenbach, and D. Yagan. How does your kindergarten classroom affect your earnings? evidence from project star. *The Quarterly journal of economics*, 126(4):1593–1660, 2011.
- [13] N. Courty, R. Flamary, and D. Tuia. Domain adaptation with regularized optimal transport. In *European Conference on Machine Learning and Principles and Practice of Knowledge Discovery in Databases*, pages 274–289, 2014.

- [14] N. Courty, R. Flamary, A. Habrard, and A. Rakotomamonjy. Joint distribution optimal transportation for domain adaptation. In *Annual Conference on Neural Information Processing Systems*, pages 3733–3742, 2017.
- [15] N. Courty, R. Flamary, A. Habrard, and A. Rakotomamonjy. Joint distribution optimal transportation for domain adaptation. *Advances in neural information processing systems*, 30, 2017.
- [16] N. Courty, R. Flamary, D. Tuia, and A. Rakotomamonjy. Optimal transport for domain adaptation. *IEEE Transactions on Pattern Analysis and Machine Intelligence*, 39(9):1853–1865, 2017.
- [17] M. Cuturi. Sinkhorn distances: Lightspeed computation of optimal transport. In *Annual Conference on Neural Information Processing Systems*, pages 2292–2300, 2013.
- [18] E. Dunipace. Optimal transport weights for causal inference. *arXiv preprint arXiv:2109.01991*, 2021.
- [19] T. R. Fleming, R. L. Prentice, M. S. Pepe, and D. Glidden. Surrogate and auxiliary endpoints in clinical trials, with potential applications in cancer and aids research. *Statistics in medicine*, 13(9):955–968, 1994.
- [20] K. Fukumizu, A. Gretton, X. Sun, and B. Schölkopf. Kernel measures of conditional dependence. *Advances in neural information processing systems*, 20, 2007.
- [21] A. Ghassami, A. Yang, D. Richardson, I. Shpitser, and E. T. Tchetgen. Combining experimental and observational data for identification and estimation of long-term causal effects. *arXiv preprint arXiv:2201.10743*, 2022.
- [22] A. Gretton, O. Bousquet, A. Smola, and B. Schölkopf. Measuring statistical dependence with hilbert-schmidt norms. In *International conference on algorithmic learning theory*, pages 63–77. Springer, 2005.
- [23] F. Gunsilius and Y. Xu. Matching for causal effects via multimarginal unbalanced optimal transport. *arXiv preprint arXiv:2112.04398*, 2021.
- [24] D. Guo, Z. Li, H. Zhao, M. Zhou, H. Zha, et al. Learning to re-weight examples with optimal transport for imbalanced classification. *Advances in Neural Information Processing Systems*, 35:25517–25530, 2022.
- [25] H. Hohnhold, D. O’Brien, and D. Tang. Focusing on the long-term: It’s good for users and business. In *Proceedings of the 21th ACM SIGKDD International Conference on Knowledge Discovery and Data Mining*, pages 1849–1858, 2015.
- [26] W. Hu, X. Zhou, and P. Wu. Identification and estimation of treatment effects on long-term outcomes in clinical trials with external observational data. *Statistica Sinica*. doi: 10.5705/ss.202023.0006.
- [27] G. Imbens, N. Kallus, X. Mao, and Y. Wang. Long-term causal inference under persistent confounding via data combination. *Journal of the Royal Statistical Society Series B: Statistical Methodology*, page qkae095, 10 2024. ISSN 1369-7412. doi: 10.1093/jrsssb/qkae095. URL <https://doi.org/10.1093/jrsssb/qkae095>.
- [28] G. W. Imbens. The role of the propensity score in estimating dose-response functions. *Biometrika*, 87(3):706–710, 2000.
- [29] N. Kallus and X. Mao. On the role of surrogates in the efficient estimation of treatment effects with limited outcome data. *arXiv preprint arXiv:2003.12408*, 2020.
- [30] L. V. Kantorovich. On the translocation of masses. *Journal of mathematical sciences*, 133(4): 1381–1382, 2006.
- [31] L. Kantorovitch. On the translocation of masses. *Management Science*, 5(1):1–4, 1958.

- [32] A. Kazemi and M. Ester. Adversarially balanced representation for continuous treatment effect estimation. In *Proceedings of the AAAI Conference on Artificial Intelligence*, volume 38, pages 13085–13093, 2024.
- [33] E. H. Kennedy, Z. Ma, M. D. McHugh, and D. S. Small. Non-parametric methods for doubly robust estimation of continuous treatment effects. *Journal of the Royal Statistical Society Series B: Statistical Methodology*, 79(4):1229–1245, 2017.
- [34] Y.-g. Kim, K. Lee, and M. C. Paik. Conditional wasserstein generator. *IEEE Transactions on Pattern Analysis and Machine Intelligence*, 45(6):7208–7219, 2022.
- [35] D. P. Kingma and J. Ba. Adam: A method for stochastic optimization. *arXiv preprint arXiv:1412.6980*, 2014.
- [36] Q. Li, Z. Wang, S. Liu, G. Li, and G. Xu. Causal optimal transport for treatment effect estimation. *IEEE transactions on neural networks and learning systems*, 34(8):4083–4095, 2021.
- [37] H. P. Margetic, M. El Gheche, G. Chierchia, and P. Frossard. Fgot: Graph distances based on filters and optimal transport. In *Proceedings of the AAAI Conference on Artificial Intelligence*, volume 36, pages 7710–7718, 2022.
- [38] G. Monge. Mémoire sur la théorie des déblais et des remblais. *Histoire de l’Académie Royale des Sciences de Paris*, 1781.
- [39] A. S. Nemirovskij and D. B. Yudin. Problem complexity and method efficiency in optimization. 1983.
- [40] L. Nie, M. Ye, qiang liu, and D. Nicolae. Varying coefficient neural network with functional targeted regularization for estimating continuous treatment effects. In *International Conference on Learning Representations*, 2021. URL <https://openreview.net/forum?id=RmB-88r9dL>.
- [41] F. Obradović. Identification of long-term treatment effects via temporal links, observational, and experimental data. *arXiv preprint arXiv:2411.04380*, 2024.
- [42] A. B. Owen. Monte carlo theory, methods and examples, 2013.
- [43] Y. Park and Y. Sasaki. A bracketing relationship for long-term policy evaluation with combined experimental and observational data. *arXiv preprint arXiv:2401.12050*, 2024.
- [44] G. Peyré, M. Cuturi, et al. Computational optimal transport: With applications to data science. *Foundations and Trends® in Machine Learning*, 11(5-6):355–607, 2019.
- [45] G. Raskutti and S. Mukherjee. The information geometry of mirror descent. *IEEE Transactions on Information Theory*, 61(3):1451–1457, 2015.
- [46] D. B. Rubin. Estimating causal effects of treatments in randomized and nonrandomized studies. *Journal of educational Psychology*, 66(5):688, 1974.
- [47] Y. Rubner, C. Tomasi, and L. J. Guibas. The earth mover’s distance as a metric for image retrieval. *International Journal of Computer Vision*, 40(2):99–121, 2000.
- [48] P. Schwab, L. Linhardt, S. Bauer, J. M. Buhmann, and W. Karlen. Learning counterfactual representations for estimating individual dose-response curves. In *Proceedings of the AAAI Conference on Artificial Intelligence*, volume 34, pages 5612–5619, 2020.
- [49] U. Shalit, F. D. Johansson, and D. Sontag. Estimating individual treatment effect: generalization bounds and algorithms. In *International conference on machine learning*, pages 3076–3085. PMLR, 2017.
- [50] R. Singh. Generalized kernel ridge regression for long term causal inference: Treatment effects, dose responses, and counterfactual distributions. *arXiv preprint arXiv:2201.05139*, 2022.
- [51] M. Sommerfeld, J. Schrieber, Y. Zemel, and A. Munk. Optimal transport: Fast probabilistic approximation with exact solvers. *Journal of Machine Learning Research*, 20(105):1–23, 2019.

- [52] X. Sun, D. Janzing, B. Schölkopf, and K. Fukumizu. A kernel-based causal learning algorithm. In *Proceedings of the 24th international conference on Machine learning*, pages 855–862, 2007.
- [53] E. J. Tchetgen Tchetgen, A. Ying, Y. Cui, X. Shi, and W. Miao. An introduction to proximal causal inference. *Statistical Science*, 39(3):375–390, 2024.
- [54] V. Titouan, N. Courty, R. Tavenard, and R. Flamary. Optimal transport for structured data with application on graphs. In *International Conference on Machine Learning*, pages 6275–6284. PMLR, 2019.
- [55] I. Tolstikhin, O. Bousquet, S. Gelly, and B. Schölkopf. Wasserstein auto-encoders. In *International Conference on Learning Representations*, 2018.
- [56] A. Tran, A. Bibaut, and N. Kallus. Inferring the long-term causal effects of long-term treatments from short-term experiments. In *Forty-first International Conference on Machine Learning*.
- [57] S. Tübbicke. Entropy balancing for continuous treatments. *Journal of Econometric Methods*, 11(1):71–89, 2022.
- [58] G. Van Goffrier, L. Maystre, and C. M. Gilligan-Lee. Estimating long-term causal effects from short-term experiments and long-term observational data with unobserved confounding. In *Conference on Causal Learning and Reasoning*, pages 791–813. PMLR, 2023.
- [59] B. G. Vegetabile, B. A. Griffin, D. L. Coffman, M. Cefalu, M. W. Robbins, and D. F. McCaffrey. Nonparametric estimation of population average dose-response curves using entropy balancing weights for continuous exposures. *Health Services and Outcomes Research Methodology*, 21: 69–110, 2021.
- [60] C. Villani. *Optimal transport: old and new*, volume 338. Springer Science & Business Media, 2008.
- [61] C. Villani. *Topics in optimal transportation*, volume 58. American Mathematical Soc., 2021.
- [62] C. Villani et al. *Optimal transport: old and new*, volume 338. Springer, 2009.
- [63] C. Vincent-Cuaz, R. Flamary, M. Corneli, T. Vayer, and N. Courty. Semi-relaxed gromov wasserstein divergence with applications on graphs. In *International Conference on Learning Representations*, 2022.
- [64] H. Wang, J. Fan, Z. Chen, H. Li, W. Liu, T. Liu, Q. Dai, Y. Wang, Z. Dong, and R. Tang. Optimal transport for treatment effect estimation. *Advances in Neural Information Processing Systems*, 36, 2024.
- [65] X. Wang, S. Lyu, X. Wu, T. Wu, and H. Chen. Generalization bounds for estimating causal effects of continuous treatments. *Advances in Neural Information Processing Systems*, 35: 8605–8617, 2022.
- [66] J. N. Weinstein, E. A. Collisson, G. B. Mills, K. R. Shaw, B. A. Ozenberger, K. Ellrott, I. Shmulevich, C. Sander, and J. M. Stuart. The cancer genome atlas pan-cancer analysis project. *Nature genetics*, 45(10):1113–1120, 2013.
- [67] P. Wu, Z. Shen, F. Xie, Z. Wang, C. Liu, and Y. Zeng. Policy learning for balancing short-term and long-term rewards. In *Proceedings of the 41st International Conference on Machine Learning*, pages 53817–53846, 2024.
- [68] H. Xu. Gromov-wasserstein factorization models for graph clustering. In *Proceedings of the AAAI conference on artificial intelligence*, volume 34, pages 6478–6485, 2020.
- [69] Y. Yan, H. Zhou, Z. Yang, W. Chen, R. Cai, and Z. Hao. Reducing balancing error for causal inference via optimal transport. In *Forty-first International Conference on Machine Learning*.
- [70] Y. Yan, M. Tan, Y. Xu, J. Cao, M. Ng, H. Min, and Q. Wu. Oversampling for imbalanced data via optimal transport. In *AAAI Conference on Artificial Intelligence*, volume 33, pages 5605–5612, 2019.

- [71] Y. Yan, Z. Yang, W. Chen, R. Cai, Z. Hao, and M. K.-P. Ng. Exploiting geometry for treatment effect estimation via optimal transport. In *Proceedings of the AAAI Conference on Artificial Intelligence*, volume 38, pages 16290–16298, 2024.
- [72] Q. Yang, X. Liu, Y. Zeng, R. Guo, Y. Liu, and P. Wu. Learning the optimal policy for balancing short-term and long-term rewards. *Advances in Neural Information Processing Systems*, 37: 36514–36540, 2024.
- [73] Y. Yang, X. Gu, and J. Sun. Prototypical partial optimal transport for universal domain adaptation. In *Proceedings of the AAAI Conference on Artificial Intelligence*, volume 37, pages 10852–10860, 2023.
- [74] Z. Zeng, D. Arbour, A. Feller, R. Addanki, R. Rossi, R. Sinha, and E. H. Kennedy. Continuous treatment effects with surrogate outcomes. *arXiv preprint arXiv:2402.00168*, 2024.
- [75] P. Zhao and Z.-H. Zhou. Label distribution learning by optimal transport. In *Proceedings of the AAAI Conference on Artificial Intelligence*, volume 32, 2018.
- [76] Y. Zhu, D. L. Coffman, and D. Ghosh. A boosting algorithm for estimating generalized propensity scores with continuous treatments. *Journal of causal inference*, 3(1):25–40, 2015.

## A Proof Details

### A.1 Proof of Proposition 1

**Proposition 1.** *Under Assumptions 1, 2, 3, 4, 5, and 6, given a set of weights  $\mathbf{w} = \{\mathbf{w}_o, \boldsymbol{\mu}\}$  consisting of the learnable weights  $\mathbf{w}_o$  for observational units and uniform weights  $\boldsymbol{\mu}$  for experimental units, which makes  $P^{\mathbf{w}}(\mathbf{S}, G|\mathbf{X}, A) = P^{\mathbf{w}}(\mathbf{S}|\mathbf{X}, A)P^{\mathbf{w}}(G|\mathbf{X}, A)$ , i.e.,  $\mathbf{S} \perp\!\!\!\perp G|\mathbf{X}, A$ , then  $\mathbb{E}_{P^{\mathbf{w}}}[\mathbf{S}(a)|\mathbf{X}, A = a, G = o] = \mathbb{E}_{P^{\mathbf{w}}}[\mathbf{S}(a)|\mathbf{X}, G = o]$  holds.*

*Proof.* Based on Assumption 1, we rewrite  $P^{\mathbf{w}}(\mathbf{S}, G|\mathbf{X}, A) = P^{\mathbf{w}}(\mathbf{S}|\mathbf{X}, A)P^{\mathbf{w}}(G|\mathbf{X}, A)$  as  $P^{\mathbf{w}}(\mathbf{S}(a), G|\mathbf{X}, A = a) = P^{\mathbf{w}}(\mathbf{S}(a)|\mathbf{X}, A = a)P^{\mathbf{w}}(G|\mathbf{X}, A = a)$ . Based on chain rule, we have

$$P^{\mathbf{w}}(\mathbf{S}(a), G|\mathbf{X}, A = a) = P^{\mathbf{w}}(\mathbf{S}(a)|G, \mathbf{X}, A = a)P^{\mathbf{w}}(G|\mathbf{X}, A = a), \quad (\text{A.1})$$

then we have

$$P^{\mathbf{w}}(\mathbf{S}(a)|\mathbf{X}, A = a) = P^{\mathbf{w}}(\mathbf{S}(a)|G, \mathbf{X}, A = a). \quad (\text{A.2})$$

Note that, based on Eq. (A.2), we have

$$\begin{aligned} P^{\mathbf{w}}(\mathbf{S}(a)|\mathbf{X}, A = a) &= P^{\mathbf{w}}(\mathbf{S}(a)|G, \mathbf{X}, A = a) \\ &= P^{\mathbf{w}}(\mathbf{S}(a)|G = e, \mathbf{X}, A = a), \end{aligned} \quad (\text{A.3})$$

and thus we have

$$P^{\mathbf{w}}(\mathbf{S}(a), G|\mathbf{X}, A = a) = P^{\mathbf{w}}(\mathbf{S}(a)|G = e, \mathbf{X}, A = a)P^{\mathbf{w}}(G|\mathbf{X}, A = a). \quad (\text{A.4})$$

Based on Assumption 4, we have

$$P^{\mathbf{w}}(\mathbf{S}(a), G|\mathbf{X}, A = a) = P^{\mathbf{w}}(\mathbf{S}(a)|G = e, \mathbf{X})P^{\mathbf{w}}(G|\mathbf{X}, A = a). \quad (\text{A.5})$$

Based on Assumption 5, we have

$$P^{\mathbf{w}}(\mathbf{S}(a), G|\mathbf{X}, A = a) = P^{\mathbf{w}}(\mathbf{S}(a)|G, \mathbf{X})P^{\mathbf{w}}(G|\mathbf{X}, A = a). \quad (\text{A.6})$$

Hence, based on Eq. (A.1) and (A.6), we conclude

$$P^{\mathbf{w}}(\mathbf{S}(a)|\mathbf{X}, A = a, G) = P^{\mathbf{w}}(\mathbf{S}(a)|\mathbf{X}, G), \quad (\text{A.7})$$

and thus  $\mathbb{E}_{P^{\mathbf{w}}}[\mathbf{S}(a)|\mathbf{X}, A = a, G = o] = \mathbb{E}_{P^{\mathbf{w}}}[\mathbf{S}(a)|\mathbf{X}, G = o]$  hold. □

### A.2 Proof of Theorem 1

**Theorem 1.** *Suppose assumptions in Proposition 1 hold, we have the unconfoundedness  $\mathbb{E}_{P^{\mathbf{w}}}[Y(a)|\mathbf{X}, A = a, G = o] = \mathbb{E}_{P^{\mathbf{w}}}[Y(a)|\mathbf{X}, G = o]$ , then the long-term HDRC can be identified.*

*Proof.* Firstly, we show that  $\mathbb{E}_{P^{\mathbf{w}}}[Y(a)|\mathbf{X}, A = a, G = o] = \mathbb{E}_{P^{\mathbf{w}}}[Y(a)|\mathbf{X}, G = o]$  holds based on Proposition 1. Specifically,

$$\begin{aligned} &P^{\mathbf{w}}(Y(a)|\mathbf{X}, A = a, G = o) \\ &= \int P^{\mathbf{w}}(Y(a), \mathbf{S}(a)|\mathbf{X}, A = a, G = o)d\mathbf{S}(a) \\ &= \int P^{\mathbf{w}}(Y(a)|\mathbf{S}(a), \mathbf{X}, A = a, G = o)P^{\mathbf{w}}(\mathbf{S}(a)|\mathbf{X}, A = a, G = o)d\mathbf{S}(a) \\ &= \int P^{\mathbf{w}}(Y(a)|\mathbf{S}(a), \mathbf{X}, G = o)P^{\mathbf{w}}(\mathbf{S}(a)|\mathbf{X}, G = o)d\mathbf{S}(a) \\ &= \int P^{\mathbf{w}}(Y(a), \mathbf{S}(a)|\mathbf{X}, G = o)d\mathbf{S}(a) \\ &= P^{\mathbf{w}}(Y(a)|\mathbf{X}, G = o), \end{aligned} \quad (\text{A.8})$$

where the second equality is based on the chain rule, the third equality is based on Assumption 6 and Eq. (A.7). Based on the above equality, we can directly conclude

$$\mathbb{E}_{P^w}[Y(a)|\mathbf{X}, A = a, G = o] = \mathbb{E}_{P^w}[Y(a)|\mathbf{X}, G = o]. \quad (\text{A.9})$$

Then HDRC is identified:

$$\begin{aligned} \mathbb{E}_{P^w}[Y(a)|\mathbf{X} = \mathbf{x}] &= \mathbb{E}_{P^w}[Y(a)|\mathbf{X} = \mathbf{x}, G = o] \\ &= \mathbb{E}_{P^w}[Y(a)|\mathbf{X} = \mathbf{x}, A = a, G = o] \\ &= \mathbb{E}_{P^w}[Y|\mathbf{X} = \mathbf{x}, A = a, G = o], \end{aligned} \quad (\text{A.10})$$

where the first equality is based on Assumption 5, the second equality is based on the result of Eq. (A.9), and the third equality is based on Assumption 1.  $\square$

### A.3 Proof of Theorem 2

We firstly define the empirical observational distribution  $P(\mathbf{S}, \mathbf{X}, A|G = o)$  as  $\alpha_{\mathbf{w}_o} = \sum_{i=1}^{n_o} w_{o,i} \delta(\mathbf{s}_i, \mathbf{x}_i, a_i)$ , where  $\mathbf{w}_o$  is the to-be-learned weights, and we define the empirical experimental distribution  $P(\mathbf{S}, \mathbf{X}, A|G = e)$  as  $\beta = \sum_{i=1}^{n_e} \frac{1}{n_e} \delta(\mathbf{s}_i, \mathbf{x}_i, a_i)$ . We also have the following lemma, which states the convergence of the importance sampling weights:

**Lemma 1.** *Under the assumption of  $P(\mathbf{S} = \mathbf{s}, \mathbf{X} = \mathbf{x}, A = a|G = g) > 0$ , let the importance sampling weights as  $\check{w}_{o,i}^* = \frac{dP(\mathbf{s}_i, \mathbf{x}_i, a_i|G=e)}{dP(\mathbf{s}_i, \mathbf{x}_i, a_i|G=o)}$  and the corresponding self-normalized weights as  $w_{o,i}^* = \frac{\check{w}_{o,i}^*}{\sum_i \check{w}_{o,i}^*}$ . Then we have  $P(\lim_{n_o \rightarrow \infty} \alpha_{\mathbf{w}_o^*} = \beta) = 1$ .*

Based on Theorem 9.2 in [42], Lemma 1 is easy to establish by viewing  $\delta(\mathbf{s}_i, \mathbf{x}_i, a_i)$  as the function of interest  $f(\cdot)$  in the importance sampling.

Now we are ready to prove Theorem 2.

**Theorem 2.** *Assuming the cost matrix of the joint distribution  $P(\mathbf{S}, \mathbf{X}, A)$  is separable, i.e.,  $C(\mathbf{s}, \mathbf{x}, a; \tilde{\mathbf{s}}, \tilde{\mathbf{x}}, \tilde{a}) = C(\mathbf{s}; \tilde{\mathbf{s}}) + C(\mathbf{x}; \tilde{\mathbf{x}}) + C(a; \tilde{a})$ , we have:*

$$OT_{\mathbf{x},a}^{con} \leq OT(P(\mathbf{S}, \mathbf{X}, A|G = o), P(\mathbf{S}, \mathbf{X}, A|G = e)),$$

*In addition, with assumption  $P(\mathbf{S} = \mathbf{s}, \mathbf{X} = \mathbf{x}, A = a|G = g) > 0$ , we have  $OT(P(\mathbf{S}, \mathbf{X}, A|G = o), P(\mathbf{S}, \mathbf{X}, A|G = e)) \rightarrow 0$  as  $n_o \rightarrow \infty$ , leading to  $OT_{\mathbf{x},a}^{con} \rightarrow 0$ .*

*Proof.* With the separable assumption of the cost matrix, we abbreviate the cost matrix about the joint distribution  $P(\mathbf{S}, \mathbf{X}, A)$  as  $C_{\mathbf{s},\mathbf{x},a} = C_{\mathbf{s}} + C_{\mathbf{x}} + C_a$ . Then for any  $\Gamma_{\mathbf{s},\mathbf{x},a,\tilde{\mathbf{s}},\tilde{\mathbf{x}},\tilde{a}} \in \Pi(P(\mathbf{S}, \mathbf{X}, A|G = o), P(\mathbf{S}, \mathbf{X}, A|G = e))$ , we have:

$$\begin{aligned} &OT(P(\mathbf{S}, \mathbf{X}, A|G = o), P(\mathbf{S}, \mathbf{X}, A|G = e)) \\ &= \min_{\Gamma} \langle \Gamma_{\mathbf{s},\mathbf{x},a,\tilde{\mathbf{s}},\tilde{\mathbf{x}},\tilde{a}}, C_{\mathbf{s},\mathbf{x},a} \rangle \\ &= \min_{\Gamma} \langle \Gamma_{\mathbf{s},\mathbf{x},a,\tilde{\mathbf{s}},\tilde{\mathbf{x}},\tilde{a}}, C_{\mathbf{s}} + C_{\mathbf{x}} + C_a \rangle \\ &\geq \min_{\Gamma} \langle \Gamma_{\mathbf{s},\mathbf{x},a,\tilde{\mathbf{s}},\tilde{\mathbf{x}},\tilde{a}}, C_{\mathbf{s}} \rangle \\ &\geq \min_{\Gamma} \langle \Gamma_{\mathbf{s},\mathbf{x},a,\tilde{\mathbf{s}},\tilde{\mathbf{x}},\tilde{a}} \mathbb{I}(\mathbf{x} = \tilde{\mathbf{x}}, a = \tilde{a}), C_{\mathbf{s}} \rangle \\ &= \min_{\Gamma} \sum_{\mathbf{x},a,\tilde{\mathbf{x}},\tilde{a}} \mathbb{I}(\mathbf{x} = \tilde{\mathbf{x}}, a = \tilde{a}) \langle \Gamma_{\mathbf{s}|x,a,\tilde{\mathbf{s}}|\tilde{\mathbf{x}},\tilde{a}}, C_{\mathbf{s}} \rangle \\ &= \min_{\Gamma} \sum_{\mathbf{x},a} \langle \Gamma_{\mathbf{s}|\mathbf{x},a,\tilde{\mathbf{s}}|\mathbf{x},a}, C_{\mathbf{s}} \rangle \\ &= OT_{\mathbf{x},a}^{con}. \end{aligned}$$

Next, we establish the convergence property. Recall that the definition of  $\hat{\mathbf{w}}_o = \min_{\mathbf{w}_o} OT(P(\mathbf{S}, \mathbf{X}, A|G = o), P(\mathbf{S}, \mathbf{X}, A|G = e)) = \min_{\mathbf{w}_o} OT(\alpha_{\mathbf{w}_o}, \beta)$ , we have  $OT(\alpha_{\hat{\mathbf{w}}_o}, \beta) \leq OT(\alpha_{\mathbf{w}_o^*}, \beta)$ . Based on Lemma 1, when  $n_o \rightarrow \infty$ , we could obtain:

$$\begin{aligned} \alpha_{\mathbf{w}_o^*} \rightarrow \beta &\implies OT(\alpha_{\mathbf{w}_o^*}, \beta) \rightarrow 0 \\ &\implies OT(\alpha_{\hat{\mathbf{w}}_o}, \beta) \rightarrow 0, \end{aligned}$$

which means that with the estimated weights  $\hat{\mathbf{w}}_o$ , we have  $OT(P(\mathbf{S}, \mathbf{X}, A|G = o), P(\mathbf{S}, \mathbf{X}, A|G = e)) \rightarrow 0$ . Therefore, we also have  $OT_{\mathbf{x},a}^{con} \rightarrow 0$ , since it is the lower bound of  $OT(P(\mathbf{S}, \mathbf{X}, A|G = o), P(\mathbf{S}, \mathbf{X}, A|G = e))$ .  $\square$

#### A.4 Proof of Theorem 3

**Theorem 3.** *Let  $\gamma_i$  be the optimal transport probability matrix of the  $i$ -th batch OT problem of  $m$ -OT( $P(\mathbf{S}, \mathbf{X}, A|G = o), P(\mathbf{S}, \mathbf{X}, A|G = e)$ ), i.e.,  $OT(P_{\mathcal{B}_i}(\mathbf{S}, \mathbf{X}, A|G = o), P(\mathbf{S}, \mathbf{X}, A|G = e))$ . We extend  $\gamma_i$  to a  $n_o \times n_e$  matrix  $\Gamma_i$  that pads zero entries to the row whose index does not belong to  $\mathcal{B}_i$ , then we have:*

$$\frac{1}{k} \sum_{i=1}^k \Gamma_i \in \Pi(P(\mathbf{S}, \mathbf{X}, A|G = o), P(\mathbf{S}, \mathbf{X}, A|G = e)), \quad (\text{A.11})$$

and

$$OT(P(\mathbf{S}, \mathbf{X}, A|G = o), P(\mathbf{S}, \mathbf{X}, A|G = e)) \leq m\text{-}OT(P(\mathbf{S}, \mathbf{X}, A|G = o), P(\mathbf{S}, \mathbf{X}, A|G = e)). \quad (\text{A.12})$$

*Proof.* Assuming the probability measure of  $P(\mathbf{S}, \mathbf{X}, A|G = o)$  and  $P(\mathbf{S}, \mathbf{X}, A|G = e)$  are  $\alpha, \beta$ , respectively. Then according to the definition, the proof of Eq. (A.11) is equivalent to prove:

$$\left( \frac{1}{k} \sum_{i=1}^k \Gamma_i \right) \mathbf{1}_{n_e} = \alpha, \quad \left( \frac{1}{k} \sum_{i=1}^k \Gamma_i \right)^T \mathbf{1}_{n_o} = \beta.$$

Note that  $\gamma_i \in \Pi(P_{\mathcal{B}_i}(\mathbf{S}, \mathbf{X}, A|G = o), P(\mathbf{S}, \mathbf{X}, A|G = e))$  satisfies:

$$\gamma_i \mathbf{1}_{n_e} = \alpha_{\mathcal{B}_i}, \quad \gamma_i^T \mathbf{1}_b = \beta.$$

Combining it with the definition of  $\Gamma_i$ , we have:

$$\Gamma_i \mathbf{1}_{n_e} = \bar{\alpha}_{\mathcal{B}_i} = \eta_i \odot \alpha, \quad (\text{A.13})$$

$$\Gamma_i^T \mathbf{1}_{n_o} = \beta, \quad (\text{A.14})$$

where  $\bar{\alpha}_{\mathcal{B}_i} \in \mathbb{R}^{n_o}$  is the extension of  $\alpha_{\mathcal{B}_i}$  by padding zero entries to the dimension whose index does not belong to  $\mathcal{B}_i$ ,  $\odot$  corresponds to entry-wise product and  $\eta_i$  is a  $n_o$  dimensional vector with element satisfying that:

$$\eta_i^j = \begin{cases} \frac{n_o}{b} = k, & \text{if } j \in \mathcal{B}_i, \\ 0, & \text{otherwise.} \end{cases} \quad (\text{A.15})$$

According Eq. (A.13) and (A.14), we have:

$$\begin{aligned} \left( \frac{1}{k} \sum_{i=1}^k \Gamma_i \right) \mathbf{1}_{n_e} &= \frac{1}{k} \sum_{i=1}^k (\Gamma_i \mathbf{1}_{n_e}) = \left( \frac{1}{k} \sum_{i=1}^k \eta_i \right) \odot \alpha, \\ \left( \frac{1}{k} \sum_{i=1}^k \Gamma_i \right)^T \mathbf{1}_{n_o} &= \frac{1}{k} \sum_{i=1}^k (\Gamma_i^T \mathbf{1}_{n_o}) = \frac{1}{k} \sum_{i=1}^k \beta = \beta, \end{aligned} \quad (\text{A.16})$$

Combining Eq. (A.15) with conditions  $\mathcal{B}_i \cap \mathcal{B}_j = \emptyset$  and  $\cup_{i=1}^k \mathcal{B}_i = \{1, 2, \dots, n_o\}$ , we obtain that:

$$\left( \frac{1}{k} \sum_{i=1}^k \eta_i \right)^j = k \sum_{i=1}^k \mathbb{I}(j \in \mathcal{B}_i) = k,$$

which means that the term  $\frac{1}{k} \sum_{i=1}^k \eta_i$  in Eq. (A.16) is  $\frac{1}{k} \sum_{i=1}^k \eta_i = \mathbf{1}_{n_o}$ . As a result, we have already proved Eq. (A.11) because the following definition holds:

$$\left( \frac{1}{k} \sum_{i=1}^k \Gamma_i \right) \mathbf{1}_{n_e} = \alpha, \quad \left( \frac{1}{k} \sum_{i=1}^k \Gamma_i \right)^T \mathbf{1}_{n_o} = \beta.$$

By denoting the cost matrix between  $P(\mathbf{S}, \mathbf{X}, A|G = o)$  and  $P(\mathbf{S}, \mathbf{X}, A|G = e)$  as  $C$ , the above definition also leads to the following inequality:

$$\begin{aligned}
& OT(P(\mathbf{S}, \mathbf{X}, A|G = o), P(\mathbf{S}, \mathbf{X}, A|G = e)) \\
& \leq \left\langle \frac{1}{k} \sum_{i=1}^k \Gamma_i, C \right\rangle = \frac{1}{k} \sum_{i=1}^k \langle \Gamma_i, C \rangle \\
& = \frac{1}{k} \sum_{i=1}^k OT(P_{\mathcal{B}_i}(\mathbf{S}, \mathbf{X}, A|G = o), P(\mathbf{S}, \mathbf{X}, A|G = e)) \tag{A.17} \\
& = m\text{-}OT(P(\mathbf{S}, \mathbf{X}, A|G = o), P(\mathbf{S}, \mathbf{X}, A|G = e)),
\end{aligned}$$

where the Eq. (A.17) comes from the definition of  $\Gamma_i$ . So far, we have finished the proof of Eq. (A.12).  $\square$

### A.5 Proof of Theorem 4

**Theorem 4.** Assuming a family  $\mathcal{M}$  of function  $m : \mathcal{Z} \times \mathcal{A} \rightarrow \mathbb{R}$ , and there exists a constant  $B_\phi > 0$  such that  $\frac{1}{B_\phi} \cdot \ell_{\phi, g, h}(\mathbf{x}, a) \in \mathcal{M}$ , then we have:

$$\mathcal{E}_{cf} \leq \mathcal{E}_f^{\mathbf{w}_o} + IPM_{\mathcal{M}}(P(\mathbf{Z})P(A), \mathbf{w}_o \cdot P(\mathbf{Z}, A)),$$

where  $IPM_{\mathcal{M}}(p, q) = \sup_{m \in \mathcal{M}} \left| \int_{\mathcal{X}} g(x)(p(x) - q(x))dx \right|$  is integral probability metric for a chosen  $\mathcal{M}$ ,  $P(\mathbf{Z})$  and  $P(\mathbf{Z}, A)$  are distributions induced by the map  $\phi$  from  $P(\mathbf{X})$  and  $P(\mathbf{X}, A)$ .

*Proof.* The inequality is equivalent to

$$\begin{aligned}
& \mathcal{E}_{cf} - \mathcal{E}_f^{\mathbf{w}_o} \\
& = \int_{\mathcal{X}} \int_{\mathcal{A}} P(\mathbf{x})P(a)\ell_{\phi, g, h}(\mathbf{x}, a) d\mathbf{x}da - \int_{\mathcal{X}} \int_{\mathcal{A}} P^{\mathbf{w}_o}(\mathbf{x}, a)\ell_{\phi, g, h}(\mathbf{x}, a) d\mathbf{x}da \\
& = \int_{\mathcal{X}} \int_{\mathcal{A}} (P(\mathbf{x})P(a) - P^{\mathbf{w}_o}(\mathbf{x}, a)) \ell_{\phi, g, h}(\mathbf{x}, a) d\mathbf{x}da \\
& = \int_{\mathcal{Z}} \int_{\mathcal{A}} (P(\mathbf{z})P(a) - P^{\mathbf{w}_o}(\mathbf{z}, a)) \ell_{\phi, g, h}(\psi(\mathbf{z}), a) d\mathbf{z}da \tag{A.18}
\end{aligned}$$

$$\begin{aligned}
& \leq \sup_{m \in \mathcal{M}} \left| \int_{\mathcal{Z}} \int_{\mathcal{A}} (P(\mathbf{z})P(a) - P^{\mathbf{w}_o}(\mathbf{z}, a)) m(\mathbf{z}, a) d\mathbf{z}da \right| \tag{A.19} \\
& = IPM_{\mathcal{M}}(P(\mathbf{Z})P(A), P^{\mathbf{w}_o}(\mathbf{Z}, A)) \\
& = IPM_{\mathcal{M}}(P(\mathbf{Z})P(A), \mathbf{w}_o \cdot P(\mathbf{Z}, A)),
\end{aligned}$$

where Eq. (A.18) can be obtained by the standard change of variables formula, using the determinant of the Jacobian of  $\psi(\mathbf{z})$ , Eq. (A.19) is according to the definition of IPM with the assumption that  $\frac{1}{B_\phi} \cdot \ell_{\phi, g, h}(\mathbf{x}, a) \in \mathcal{M}$ .  $\square$

### A.6 Derivation about Projected Mirror Descent

In this section, following [71], we develop a projected mirror descent [39, 45] based on the Kullback-Leibler (KL) divergence to solve the following problem, which is non-trivial to address because of the equality constraints:

$$\begin{aligned}
& \min_{\mathbf{w}_{o, \mathcal{B}}} \min_{\gamma \in \Pi(\alpha_{\mathcal{B}}, \beta)} \langle \gamma, \mathbf{C} \rangle + \lambda_e \Omega(\gamma), \\
& \text{s.t. } \Pi(\alpha_{\mathcal{B}}, \beta) = \{\gamma \in \mathbb{R}^{b \times n_e} | \gamma \mathbf{1}_{n_e} = \mathbf{w}_{o, \mathcal{B}}, \gamma^T \mathbf{1}_b = \boldsymbol{\mu}, \gamma_{ij} \in [0, 1]\},
\end{aligned}$$

Firstly, we rewrite the constrain about  $\gamma$  as

$$\Pi'(\alpha_{\mathcal{B}}, \beta) = \{\gamma \in \mathbb{R}^{b \times n_e} | \gamma^T \mathbf{1}_b = \boldsymbol{\mu}, \gamma_{ij} \in [0, 1]\}, \tag{A.20}$$

which does not consider the constraint  $\gamma \mathbf{1}_{n_e} = \mathbf{w}_{o,B}$  since  $\mathbf{w}_{o,B}$  are also parameters to be optimized. Based on this, the OT problem with a negative entropy regularization is given as follows:

$$\min_{\gamma} \langle \gamma, \mathbf{C} \rangle + \lambda_e \Omega(\gamma), \quad s.t. \gamma \in \Pi'(\alpha_B, \beta). \quad (\text{A.21})$$

For simplicity, we define the objective function in Problem (A.21) as

$$f(\gamma) = \langle \gamma, \mathbf{C} \rangle + \lambda_e \Omega(\gamma),$$

and the  $(i, j)$ -th element of the gradient  $\nabla f(\gamma)$  is denoted by  $\nabla_{ij}$ ,

$$\nabla_{ij} = C_{ij} + \lambda_e \log w_i = C_{ij} + \lambda_e \log \gamma_i,$$

where  $\gamma_i$  is the sum of  $i$ -th row of  $\gamma$ . Then at each iteration, we solve the following problem:

$$\gamma^k = \min_{\gamma \in \Pi'(\alpha_B, \beta)} \eta \langle \nabla f(\gamma^{k-1}), \gamma \rangle + \mathcal{D}(\gamma \| \gamma^{k-1}), \quad (\text{A.22})$$

which firstly performs proximal gradient descent with the Bregman divergence and the stepsize  $\eta$ , and then obtains a feasible solution in the set  $\Pi'(\alpha_B, \beta)$  by projection. Next, we present the details of these two operations.

**Proximal Gradient Descent** Let  $v^k$  be the solution to Problem (A.22) without considering the constraint  $\gamma \in \Pi'(\alpha_B, \beta)$ , i.e.,

$$v^k = \min_{\gamma} \eta \langle \nabla f(\gamma^{k-1}), \gamma \rangle + \mathcal{D}(\gamma \| \gamma^{k-1}).$$

We adopt the KL divergence between two distributions  $\gamma$  and  $\gamma^{k-1}$  as the Bregman divergence  $\mathcal{D}(\gamma \| \gamma^k)$ , then the closed-form solution to the above problem is given as:

$$v^k = \gamma^{k-1} \odot \exp(-\eta \nabla f(\gamma^{k-1})). \quad (\text{A.23})$$

**Projection Operation** To make sure  $\gamma^k$  satisfies the constraints in Eq. (A.20), we update  $\gamma^k$  by finding  $\gamma \in \Pi'(\alpha_B, \beta)$  which is most close to  $v^k$  under the KL metric. This is achieved by solving the following projection problem (ignore constraint  $\gamma_{ij} \in [0, 1]$  for now):

$$\begin{aligned} \min_{\gamma} \quad & \mathcal{D}(\gamma \| v^k) = \sum_{i=1}^b \sum_{j=1}^{n_e} \gamma_{ij} \log\left(\frac{\gamma_{ij}}{v_{ij}^k}\right) - \gamma_{ij} + v_{ij}^k, \\ s.t. \quad & \gamma^\top \mathbf{1}_b = \boldsymbol{\mu}. \end{aligned} \quad (\text{A.24})$$

By introducing the Lagrangian multipliers  $\boldsymbol{\lambda} = [\lambda_1, \dots, \lambda_{n_e}]^\top$  for the equality constraint  $\gamma^\top \mathbf{1}_b = \boldsymbol{\mu}$ , we obtain the Lagrangian  $\mathcal{L}(\gamma, \boldsymbol{\lambda})$  as follows:

$$\mathcal{L}(\gamma, \boldsymbol{\lambda}) = \sum_{i=1}^b \sum_{j=1}^{n_e} \gamma_{ij} \log\left(\frac{\gamma_{ij}}{v_{ij}^k}\right) - \gamma_{ij} + v_{ij}^k + \boldsymbol{\lambda}^\top (\gamma^\top \mathbf{1}_b - \boldsymbol{\mu}).$$

By taking the partial derivative of  $\mathcal{L}(\gamma, \boldsymbol{\lambda})$  with respect to  $\gamma_{ij}$  to zero, we obtain:

$$\begin{aligned} \log \gamma_{ij} &= \log v_{ij}^k - \lambda_j \\ \Rightarrow \gamma_{ij} &= v_{ij}^k \exp(-\lambda_j). \end{aligned} \quad (\text{A.25})$$

According to the equality constraint  $\gamma^\top \mathbf{1}_b = \boldsymbol{\mu}$ , we have  $\sum_{i=1}^b \gamma_{ij} = 1/n_e$ . Combining it with the above result, we further obtain:

$$\begin{aligned} \sum_{i=1}^b \gamma_{ij} &= \sum_{i=1}^b v_{ij}^k \exp(-\lambda_j) = \exp(-\lambda_j) \sum_{i=1}^b v_{ij}^k = \frac{1}{n_e} \\ \Rightarrow \exp(-\lambda_j) &= \frac{1}{n_e \sum_{i=1}^b v_{ij}^k}. \end{aligned} \quad (\text{A.26})$$

Combining Eq. (A.25) and (A.26), we obtain the closed-form solution:

$$\gamma_{ij} = v_{ij}^k / \left( n_e \sum_{i=1}^b v_{ij}^k \right). \tag{A.27}$$

For an initial value  $\gamma_{ij}^0 \geq 0$ , given  $v_{ij}^k > 0$  which is guaranteed by the update rule in Eq. (A.20), it is obvious that the solution obtained by Eq. (A.27) satisfies the box constraint  $\gamma_{ij} \in [0, 1]$ . Therefore, Problem (A.24) does not consider this constraint explicitly.

For now, we have derived how to solve the Problem Eq. (A.21). That is, we repeat steps Eq. (A.23) and (A.27) until converging.

## B Additonal Related Work

### B.1 Dose-Response Curve Estimation

Dose-response curve estimation is broadly studied through statistical methods [59, 33, 76], and most of them are based on the Generalized Propensity Score (GPS, [28]) or the Entropy Balancing for Continuous Treatments (EBCT, [57]). Recently, deep learning-based methods also attract the attention of the research community. DRNet [48] divides the continuous treatment into several intervals, and trains one separate head for each interval. In order to produce a continuous curve, VCNet [40] adapts a varying coefficient model into neural networks to handle the continuous treatment. SCIGAN [7] generates counterfactual outcomes for continuous treatments based on the Generative Adversarial Network (GAN) framework. ADMIT [65] derives a counterfactual bound of estimating the average dose-response curve with a discretized approximation of the IPM distance, and ACFR [32] minimizes the KL-divergence using an adversarial game to extract balanced representations for continuous treatment. Different from the existing works above, we aim to estimate the HDRC under the long-term estimation scenario with unobserved confounders in this paper, which is more complex.

### B.2 Optimal Transport

Optimal transport seeks to find an optimal plan for moving mass from one distribution to another with the minimal transport cost [38, 31, 60]. Recently, optimal transport has shown powerful ability in different kinds of applications [44, 70, 75]. For computer vision, the Earth Mover’s Distance which is calculated based on the solution to the optimal transport problem, is used as a metric for image retrieval[47]. For transfer learning, data from one distribution is transported to another distribution based on the optimal transport plan for label information transfer [13, 16, 14]. For generative modeling, the Wasserstein distance derived by optimal transport is minimized to train deep generative models [55, 1]. For structured data, Wasserstein [37], Gromov-Wasserstein [68] and Fused Gromov-Wasserstein [54] are applied for graph data analysis.

Recently, there are also some works trying to introduce optimal transport into causal inference. [23] employs unbalanced optimal transport for matching. [36] proposes to infer counterfactual outcomes via transporting the factual distribution to the counterfactual one. [18, 69, 71] apply optimal transport to learn sample weights to achieve distribution balancing. [64] solves the problems of mini-batch sampling and unobserved confounders under CFR [49] framework through optimal transport. To the best of our knowledge, this is the first work exploiting optimal transport to solve the unobserved confounder problem via data combination under the long-term estimation scenario.

## C Model Details

### C.1 Implementation Details

Our code is implemented using the PyTorch 1.8.1 framework. All MLP in our model is 2 fully connected layers with 50 hidden units and Elu activation function, and we build our model as follows:

For the *balanced representation module*, we use an MLP to build the representation function  $\phi$ , and use the Wasserstein distance as the IPM term. The code of the Wasserstein distance can be found in <https://github.com/rguo12/network-deconfounder-wsdm20/blob/master/utlils.py>.

---

**Algorithm 1** Pseudocode of the proposed LEARN

---

**Require:** observational data  $O$ , experimental data  $E$ , initial model parameters  $\theta = \{\theta_\phi, \theta_q(a), \theta_g(a), \theta_f(a), \theta_h(a)\}$ , hyper-parameters  $\{\lambda_o, \lambda_b, \lambda_e\}$ , batch size  $b$ , pre-training epoch  $n_{pre}$ , training epoch  $n$ , OT epoch  $n_{ot}$ , learning rate  $\alpha$

- 1: // *Pre-training phase. Ensuring the short-term embeddings of RNN are meaningful, which will be used in constructing the cost matrix  $\mathbf{C}$  in optimal transport at each training iteration*
- 2: **for**  $i = 1, 2, \dots, n_{pre}$  **do**
- 3:     Sample a mini-batch  $\mathcal{B}$  from the observational data  $O$
- 4:     Update  $\theta^{i+1} \leftarrow \theta^i - \alpha \nabla_\theta \mathcal{L}_\theta$  by setting  $\mathbf{w}_\mathcal{B} = \{\frac{1}{b}, \frac{1}{b}, \dots, \frac{1}{b}\}$ .
- 5: **end for**
- 6: // *Training phase. Removing the observed and unobserved confounding bias*
- 7: **for**  $i = 1, 2, \dots, n$  **do**
- 8:     Sample a mini-batch  $\mathcal{B}$  from the observational data  $O$
- 9:     // *Learning weights  $\mathbf{w}_\mathcal{B}$  for the batch observational units via data combination*
- 10:     Compute the cost matrix  $\mathbf{C}$  between  $\mathcal{B}$  and  $E$
- 11:     **for**  $k = 1, 2, \dots, n_{ot}$  **do**
- 12:         Calculate  $v^k$  according to Eq. (A.23)
- 13:         Update  $\gamma^k$  according to Eq. (A.27)
- 14:     **end for**
- 15:      $\hat{\mathbf{w}}_\mathcal{B} = \gamma^{n_{ot}} \mathbf{1}_{n_e}$
- 16:     // *Weighted regression with IPM term*
- 17:     Update  $\theta^{i+1} \leftarrow \theta^i - \alpha \nabla_\theta \mathcal{L}_\theta$  by setting  $\mathbf{w}_\mathcal{B} = \hat{\mathbf{w}}_\mathcal{B}$ .
- 18: **end for**
- 19: **return** Learned model parameters  $\theta$

---

For the *OT weight module*, at each iteration, 1) We first construct the cost matrix as  $C_{ij} = \beta_r d(\bar{\mathbf{r}}_i, \bar{\mathbf{r}}_j) + \beta_x d(\mathbf{x}_i, \mathbf{x}_j) + \beta_a d(a_i, a_j)$ , where the hyperparameters  $\beta_r = 10, \beta_x = 0.1, \beta_a = 0.1$ ,  $d(\cdot, \cdot)$  is the euclidean distance, and the distance of short-term outcomes is calculated from the mean embedding of GRU as  $\bar{\mathbf{r}} = \frac{1}{t_0} \sum_{t=1}^{t_0} \mathbf{r}_t$ . As a result, we need pre-train the model firstly to ensure that the GRU's embedding is meaningful. 2) We then obtain the optimal transport probability matrix  $\gamma^*$  by repeating steps Eq. (A.23) and (A.27) until converging. 3) Finally, the weights of observational samples could be obtained as  $w_i = \sum_{j=1}^{n_e} \gamma_{ij}^*$ , where  $w_i$  is the sum of the  $i$ -th row of  $\gamma^*$ .

For the *long-term estimation module*, we use a shared MLP to build the function  $g(\cdot)$  predicting the short-term outcomes, use another MLP to build the function  $h(\cdot)$  predicting the long-term outcome, and use a GRU model to build the RNN  $q(\cdot)$  extracting the short-term representations. As for the attention mechanism  $f(\cdot)$ , we implement it as follows:

$$\tilde{\mathbf{R}}_t = \tanh(\mathbf{W}\mathbf{R}_t + \mathbf{b}), \quad \alpha_t = \frac{\exp \tilde{\mathbf{R}}_t^\top \mathbf{V}}{\sum_{t=1}^{t_0} \exp \tilde{\mathbf{R}}_t^\top \mathbf{V}}, \quad \mathbf{R}_T = \sum_{t=1}^{t_0} \alpha_t \mathbf{R}_t,$$

where  $\mathbf{W}, \mathbf{b}, \mathbf{V}$  are the parameters of the attention mechanism  $f(\cdot)$ .

Further, following [40], we model the parameters  $\theta(a)$  of the above four network structures  $q(\cdot), g(\cdot), f(\cdot), h(\cdot)$  as the varying coefficient structure, i.e.,  $\theta(a) = \sum_{l=1}^L \alpha_l \phi_l(a)$ , where  $\phi_l$  is the basis function and  $\alpha_l$  is the coefficient. Specifically, we use truncated polynomial basis with degree 2 and two knots at  $\{1/3, 2/3\}$  (altogether 5 basis) to build the varying coefficient structure. The code of the varying coefficient structure is written based on VCNet ([https://github.com/lushleaf/varying-coefficient-net-with-functional-tr/blob/main/models/dynamic\\_net.py](https://github.com/lushleaf/varying-coefficient-net-with-functional-tr/blob/main/models/dynamic_net.py)).

## C.2 Parameters Setting

We set the hyper-parameters in our model as follows: the strength of the Wasserstein distance  $\lambda_b \in \{1, 10, 50, 100\}$ , the strength of negative entropy regularization  $\lambda_e \in \{1e - 4, 1e - 2\}$ , the learning rate about the projected mirror descent as  $1e - 3$ , and the iterations about the projected mirror descent as  $\{50, 100\}$ , the strength of short-term outcome loss as  $\lambda_o \in \{0.25, 0.5, 0.75\}$ . Besides, we pre-train the model for 100 epochs without weighting, and then the number of training epochs is 400

with early stop. We use Adam [35] with learning rate of  $1e - 3$  and weight decay of  $5e - 4$ . All the experiments run on the Nvidia RTX A6000 GPU.

### C.3 Pseudocode

We provide the pseudocode of our model in Algorithm 1.

## D Experimental Details

### D.1 Dataset Generation

**Synthetic Data Generation** We simulate synthetic data as follows. For each observational unit  $i \in \{1, 2, \dots, n_o\}$  with  $G = o$ , we generate  $p$  observed covariates and  $q$  unobserved covariates from independent identical distributions, i.e.,  $X^o \sim \mathcal{N}(\mathbf{0.1}_p, \mathbf{I}_p)$  and  $U \sim \mathcal{N}(\mathbf{0.25}_q, \mathbf{I}_q)$ , where  $\mathbf{I}$  denotes the identity matrix. Similarly, we generate experimental units  $i \in \{1, 2, \dots, n_e\}$  with  $G = e$  as  $X^e \sim \mathcal{N}(\mathbf{0.2}_p, \mathbf{I}_p)$ ,  $U \sim \mathcal{N}(\mathbf{0.25}_q, \mathbf{I}_q)$ . Then we generate treatment and outcomes for two types of datasets following the causal graphs Fig. 1 with  $W_j^x \sim \mathcal{U}(0, 0.5)$ ,  $W_j^u \sim \mathcal{U}(0.2, 0.5)$ :

$$\begin{aligned} A &= \sigma \left( \sum_{j=1}^{p/3} W_j^x \sin(X_j) + \sum_{j=p/3}^{2p/3} W_j^x X_j^2 + \beta_U \bar{U} \mathbb{I}(G = o) \right), \\ S_t &= \sum_{j=p/3}^{2p/3} W_j^x X_j^2 + (t+5)A \left( \sum_{j=2p/3}^p W_j^x X_j \right) + \beta_U t A \left( \sum_{j=1}^q W_j^u \cos(U_j) \right) \\ &\quad + 0.5 \bar{S}_{1:t-1} + \mathcal{N}(0, 0.5), \quad t = 0, 1, \dots, 7 \\ Y &= 0.25 \sum_{j=1}^p W_j^x X_j^2 + \frac{A}{7} \sum_{t=1}^7 e^{1/t} S_t + \mathcal{N}(0, 0.5). \end{aligned}$$

where  $n_o = 10000$ ,  $n_e = 500$ ,  $p = 15$ ,  $q = 5$ . Besides, we design 5 synthetic datasets with varying  $\beta_U \in \{1, 1.5, 2, 2.5, 3\}$  that controls different strengths of unobserved confounding bias.

**Semi-synthetic Data Generation** For the semi-synthetic datasets, we select the News [48] and The Cancer Genome Atlas (TCGA) [66]. The News comprises 5,000 randomly sampled articles from the NY Times corpus, including media consumer opinions, and was originally introduced as a benchmark for counterfactual inference with two treatment options. The TCGA includes gene expression data from 9,659 individuals across various cancer types, enabling the estimation of cancer recurrence risk under different treatments (e.g., medication, chemotherapy, and surgery) with dosage parameters. In these semi-synthetic datasets, we reuse the original covariates. We first randomly partition the dataset into observational ( $G = o$ ) and experimental ( $G = e$ ) subsets at a 9:1 ratio, followed by segregation of original covariates into observed ( $X$ ) and unobserved ( $U$ ) ones at an 8:2 ratio. Then we follow [40, 65] to generate the assigned treatments and corresponding outcomes. After generating a set of parameters  $\mathbf{v}_{i,x} = \mathbf{u}_{i,x} / \|\mathbf{u}_{i,x}\|$  for  $i = 1, 2, 3$  (resp.,  $\mathbf{v}_{i,u}$ ), where  $\mathbf{u}_{i,x}$  (resp.,  $\mathbf{u}_{i,u}$ ) is sampled from a normal distribution  $\mathcal{N}(\mathbf{0}, \mathbf{1})$ , we have:

$$\begin{aligned} A &\sim \text{Beta}(\gamma, \beta), \text{ where } \gamma = 2, \beta = \frac{\gamma - 1}{d^*} + 2 - \gamma \text{ and } d^* = \left| \frac{\mathbf{v}_{3,x}^T X}{2\mathbf{v}_{2,x}^T X} + \frac{\mathbf{v}_{3,u}^T U}{2\mathbf{v}_{2,u}^T U} \mathbb{I}(G = o) \right|, \\ S'_t &= \max \left( -2, \min \left( 2, \exp \left( \frac{\mathbf{v}_{2,x}^T X}{\mathbf{v}_{3,x}^T X} + \frac{\mathbf{v}_{2,u}^T U}{\mathbf{v}_{3,u}^T U} - 0.3 \right) \right) \right) + \alpha t (\mathbf{v}_{1,x}^T X + \mathbf{v}_{1,u}^T U), \quad t = 0, 1, \dots, 7, \\ S_t &= 8(A - 0.5)^2 \sin \left( \frac{\pi}{2} A \right) S'_t + 0.5 \bar{S}_{1:t-1} + \mathcal{N}(0, 0.5), \\ Y &= \lambda (\mathbf{v}_{1,x}^T X + \mathbf{v}_{2,x}^T X) + \frac{A}{7} \sum_{t=1}^7 e^{1/t} S_t + \mathcal{N}(0, 0.5). \end{aligned}$$

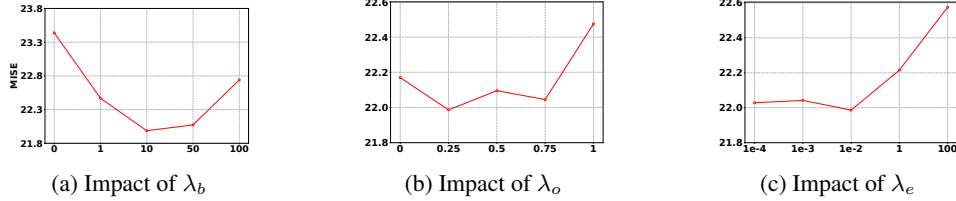


Figure 1: Hyperparameter sensitivity. (a) Strength of IPM. (b) Strength of short-term loss between observational and experimental datas. (c) Strength of negative entropy regularization.

For News, we select  $\alpha = 1, \lambda = 5$ , and for TCGA, we select  $\alpha = 20, \lambda = 50$ .

## D.2 Hyperparameter Sensitivity Study (RQ5)

We investigate the impact of three hyperparameters  $\lambda_b, \lambda_o, \lambda_e$  in Fig. 1. Firstly, we observe that MISE increases when  $\lambda_b$  becomes small or large, indicating that there exists a trade-off between balancing representation and accurate outcome estimation. Secondly, the results of varying  $\lambda_o$  shows that considering the short-term outcomes of observational and experimental datas together can bring improvement. Finally, applying the negative entropy regularization in OT is beneficial, however, MISE increases when  $\lambda_e \geq 1$ , since large  $\lambda_e$  will push the learned weights close to the uniform distribution, resulting in a failure of alignment.

## E Limitations

While our framework allows for unobserved confounders in observational data, identification still requires additional assumptions. The most critical among them is the *latent unconfoundedness* assumption, which posits that unobserved confounders affect the long-term outcome only through short-term outcomes. This assumption is reasonable in our vocational training example, where short-term skill assessments can reasonably capture unobserved confounders like learning aptitude. However, it may not hold in all real-world scenarios.

Additionally, our approach relies on Optimal Transport (OT) to learn sample weights. While OT offers several advantages, it also imposes limitations about the scalability of our method in high-dimensional or data-limited settings. First, the sample complexity of our OT-based weighting method scales as  $O(n^{-1/d})$  ( $d$  is the sum of dimensions of covariates, short-term outcomes, and treatments), which may be a little slow in high-dimensional setting. Second, Theorem 2 shows that we could only completely remove the unobserved confounding bias when we have infinite observational data. Therefore, with limited observational data, our method may only substantially reduce, but not entirely eliminate the unobserved confounding bias.

## F Broader Impact

This paper studies the problem of estimating the long-term HDRC, which utilizes the power of deep learning and optimal transport technologies to assist better long-term decision-making in many domains. For example, in a ride-hailing platform, the platform needs to evaluate the effect of various incomes of different drivers on their retention after one year to keep the long-term balance of demand and supply. In the medical field, a healthcare institution might need to analyze the impact of a new medication on the five-year survival rates of cancer patients to determine whether to adopt it as a standard treatment protocol. However, this technology towards better estimating and understanding long-term HDRC can be used negatively, where someone wishing to cause harm can use the estimated outcomes to select the worst outcome.